University of Denver

Digital Commons @ DU

Electronic Theses and Dissertations

Graduate Studies

3-1-2014

Parameter Identification of Micro-Grid Control System

Ning Gao
University of Denver

Follow this and additional works at: https://digitalcommons.du.edu/etd

Part of the Electrical and Computer Engineering Commons

Recommended Citation

Gao, Ning, "Parameter Identification of Micro-Grid Control System" (2014). *Electronic Theses and Dissertations*. 225.
https://digitalcommons.du.edu/etd/225

Parameter Identification of Micro-grid Control System

_____

A Thesis

Presented to

The faculty of Daniel Felix Ritchie School and Engineering and Computer Science

University of Denver

_____

In Partial Fulfillment

of the Requirements for the Degree

Master of Science

_____

by

Ning Gao

March 2014

Advisor: David Wenzhong Gao

Author: Ning Gao
Title: System Identification of Micro-grid
Advisor: David Wenzhong Gao
Degree Date: March 2014

Abstract

Micro-grid provides an effective means of integrating distributed energy resource (DER) units into the power systems. A micro-grid is defined as an independent low- or medium-voltage distribution network comprising various DER units, power-electronic interfaces, controllable loads, and monitoring and protection devices. Following the development of the renewable energy, micro-grid has attracted much attention.

This thesis emphasizes on the parameter identification of the control system of the micro-grid. The control system plays an important role in the stable operation of the micro-grid. The micro-grid has two operation modes, which are grid-connected operation mode and islanded operation mode. The transition between two operation modes of the micro-grid often occurs according to the condition of the entire grid. In order to make this process smooth, the control system is crucial, and the parameters of the control system is critical to the disturbance suppression during the process of transition.

In the thesis, a method combining least square method with Newton-Raphson algorithm is proposed. In order to prove the utility of the method, the parameter identification of a typical control system and its several separated elements are simulated in MATLAB. This method can identify multiple parameters at the same time and have fast convergence.

Acknowledgements

I would like to personally thank the following people who supported me with my sincere gratitude. Without their help, the thesis cannot be accomplished.

To my thesis advisor Dr. David Wenzhong Gao and his assistant Dr. Yan Li, for their precious advices to the thesis work.

To all the committee members Dr. Mohammad Matin, Dr. Jun Jason Zhang, and Dr. Stephen Sewalk, for their service and suggestions.

To all the friends around me, for their continuous encouragement.

Table of Contents

Chapter 1: Introduction

Micro-grid provides an effective means of integrating DER units into the power systems [1]. A micro-grid is defined as an independent low- or medium-voltage distribution network comprising various DER units, power-electronic interfaces, controllable loads, and monitoring and protection devices [2]. It is an autonomous system which can realize self-controlling, self-protection, and self-management. A micro-grid system can run in the islanded operation mode or the grid-connected operation mode, which makes the conventional power grid more flexible and reliable [3]. The micro-sources in a micro-grid are generally located near the customers' loads, and controlled by power electronic interfaces. The micro-grid system is connected to the external grid by interfacing devices such as bidirectional AC/DC converters. The micro-grid flow and voltage controllers regulate the flow and the bus voltage within allowable ranges. When loads change, the local micro-grid regulates the output power by itself. During the normal operation mode, the micro-grid and the external grid are running in parallel. Therefore, the micro-grid can be considered as a constant load via proper controlling. When the faults appear in the external grid or the power quality cannot satisfy the requirement, the micro-grid can enter the islanded operation mode through the controlling of interfacing devices. After the faults are cleared, the micro-grid needs to synchronize with the

external grid smoothly. Micro-grid's development and extension makes contribution to the large-scale integration of distributed sources and renewable energy sources. It enhances the reliability of power supply by various kinds of energy form and achieves the operation of active distribution network.

In recent years, some developed countries and regions (e.g., Europe, Japan, America, etc.) have studied and developed the micro-grid technologies for a period of time and have obtained some achievements. However, there are still many issues needing to be solved. These issues can be discussed from the following perspectives: micro-sources, control and protection, influence on the main grid, identification.

1.1 Micro-source

1.1.1 Distributed Sources and Distributed Energy Storage Technologies

Distributed sources mainly contain renewable energy generation systems, such as photovoltaic generation, wind generation, fuel-cell, battery, micro gas turbine and internal combustion engine [4,5]. Renewable energy is generally dispersal and has small scale. It is also limited by the natural factors. For example, sunshine or wind can generate power, but unlike fossil fuel, they cannot last all the time. So its spare energy needs to be stored by energy storage devices. Further, distributed generation based on inverters does not have enough inertia to satisfy the requirement of instantaneous power change.

Therefore, energy storage devices are necessary for the micro-grid with large number of micro-sources to keep the power balance. The energy storage technologies mainly consist of superconducting magnetic energy storage (SMES), battery energy storage, super capacitor energy storage, and flywheel energy storage [6].

The method of energy storage needs to be selected based on the requirement of system stability. For example, we can install energy storage batteries or super capacitors on the DC buses of each micro-source, or we can directly connect the micro-sources to the AC energy storage devices such as AC batteries or flywheels with inverters. The micro-grid studied by the Consortium for Electric Reliability Technology Solutions (CERTS) has DC energy storage devices installed on the DC buses of every micro-source to maintain its reliability [7]. There is also a standby source to ensure the normal operation of the micro-grid in case of the fault of components.

1.1.2 Power Electronic Interface

Micro-sources are generally connected or disconnected with the micro-grid by power electronic devices. Power electronic devices provide every distributed generation unit with the control interface.

Most of distributed generation devices need inverters, rectifiers, and filters when connecting with AC power system. The main controls of distributed generation inverter

contains inner-loop current/voltage control loop, outer-loop active/reactive power control loop, distributed and external grid synchronized control, protection and short circuit current suppression. Through the analysis of the simplified model of distributed generation interface device and based on close-loop control of the output current of voltage source inverters, the following conclusion can be drawn. When the system frequency is lower than the bandwidth of the inverters' current controllers, the distributed generation system can be treated as a voltage source, whereas when the system frequency is higher than the bandwidth of the inverters' current controllers, the distributed generation system can be treated as a current source [8].

Static switches play a very important role in the interface connecting the micro-grid with the external grid. The micro-grid study report of CERTS indicated that the static switch is to separate the sensitive loads from the grid when some serious faults begin to appear, and the micro-grid itself is still connected with the external grid. If several sources can run in synchronous operation mode, the active power direction is always from the high frequency sources to the low frequency sources before synchronization [9]. If the micro-grid and the external grid are in parallel operation, frequencies, voltage magnitudes, and phase angles need to be detected to observe the difference across the switch, and then initiate the synchronization process once the synchronization criteria is satisfied.

1.2 Control and Protection

1.2.1 Control

The conventional grid can store a great amount of energy by inertia of generators' rotors, and the inertia makes the system respond well to the loads fluctuation. Whereas, the control of the micro-grid is mostly based on power electronic technologies, so the sources' ability of anti-disturbance is very low due to the insufficient inertia [10]. Especially in the islanded operation mode, all the loads need to be balanced by distributed generation units. Therefore, the micro-grid stability becomes an important problem. Furthermore, the conventional grid has dispatching and controlling centers to keep the coordination of the whole system, but for the micro-grid, it is very difficult to locate a central control point to realize the fast reaction and control. The control of the micro-grid should be based on the local information. So how to properly coordinate and control every distributed generation unit within a micro-grid is the key to maintain the security and the reliability of a micro-grid. Especially, voltage control and frequency control should be focused on [11]. The theory of it is the same as the one of the conventional grid, which is the rational control of active power and reactive power. At present, there are two controlling methods. One is based on frequency-real power (f-P) and voltage-reactive power (V-Q) droop curve; and the other is the module control, in which the active power and reactive power is controlled by different control modules, respectively. The control of the micro-grid provides additional service to the system, e.g., active power and reactive power matching, energy utility optimization, power quality

control, protection and current suppression, communication and coordination, self-inspection and master-slave control, etc.

Unified controllers can be adopted for a multi bus micro-grid system. This kind of controllers and each distributed generation system all contain the control loop which can regulate the inner current/voltage loop and outer power loop of the three phase grid-connected inverter. The controller can be used to control the active/reactive power flow and the power sharing of each distributed generation unit in the islanded operation mode. Distributed generation controllers can control the active power and reactive power of the distributed generation units. The controlling and management of them are based on the signal measured locally, so the communication with external systems may not be necessary. Of course, whether the communication channel is needed or not finally depends on the type of controllers.

1.2.2 Protection

The emergence of the distributed generation and the micro-grid make the radial distributed network become widely used between sources and customers. The power flows are no longer only from the substation bus to the loads. It brings a big change to the setting of protective relaying and the protection mechanism [12].

The micro-grid protection approach should deal with the protection problems of all kinds of faults in two operation modes [13]. CERTS micro-grid is connected with the external grid by the static switch which can break and isolate all the faults. When breaking the faults in the micro-grid, the method should not be based on the large fault current (over-current protection). CERTS suggests that protective function should be a plug and play part of the source [14].

The connection mode of the grid-connected transformer of the distributed source has direct influences on the overvoltage and protection devices of the external grid. The synchronous machines and induction machines in the distribution system also have some influence on the setting of protection relaying. Via the analysis of the coordination of fuse, auto-reclosure, and relay, the result indicates that proper coordination relies on the capacity and the placement of the distributed generation units.

The grounding problem of the micro-grid should deal with the fault currents in the two operation modes. TN grounding systems, TT grounding systems and IT grounding systems are three families of grounding systems distinguished by International Electrotechnical Commission (IEC). The first letter indicates the connection between earth and generators or transformers. The second letter indicates the connection between earth and loads. The letter 'T' represents direct connection of a point with earth. The letter 'I' represents that no points are connected with earth, except perhaps via a high impedance. The letter 'N' represents direct connection to neutral lines, which is

connected to the earth [15]. TN grounding systems can be divided into TN-C grounding systems and TN-S grounding systems, which appear in Fig. 1.1 and Fig. 1.2, respectively. In TN-C grounding systems, the protective earth (PE) line and the neutral (N) line are combined. Whereas in TN-S grounding system, PE line and N line are separated from each other. TN-C-S grounding systems are the combination of TN-C grounding systems and TN-S grounding systems, which appears in Fig. 1.3. The TT grounding system appears in Fig. 1.4. The IT grounding system appears in Fig. 1.5. TN-C-S grounding system and TT grounding system are the most suitable grounding modes for the micro-grid neutral point [9, 16]. The parasitic resistance of the distributed system can be used to inspect whether the distributed generation system is properly grounded or not. This new technology provides the reliable, sensitive, fast protection to the incorrect grounding of distributed generation system.
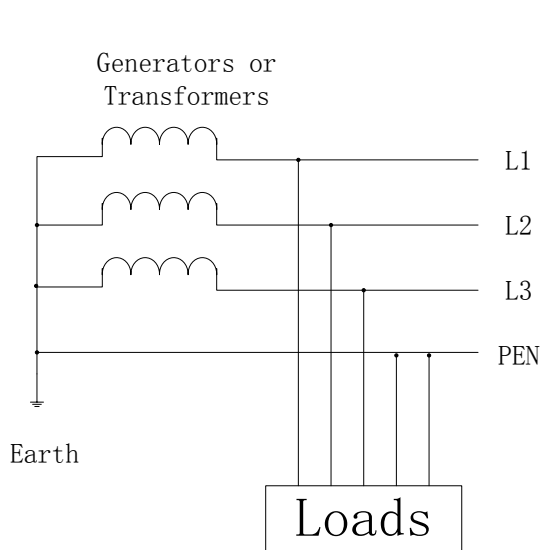
Figure 1.1 TN-C grounding system [16]   Figure 1.2 TN-S grounding system [16]
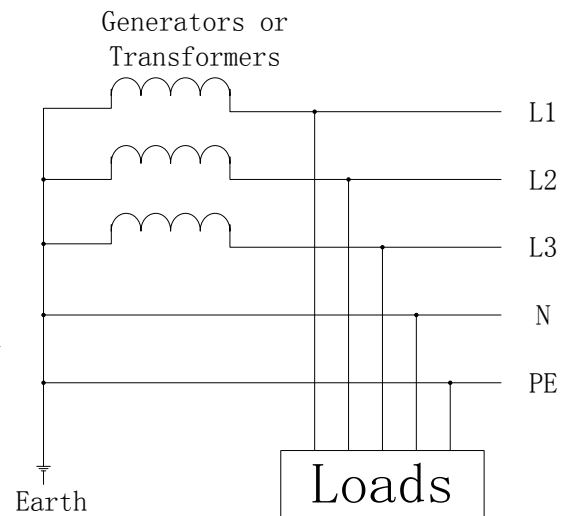
Generators or
Transformers

L1

L2

L3

N

PE

Loads

Earth

Generators or
Transformers

L1

L2

L3

N

Earth

Loads

Earth
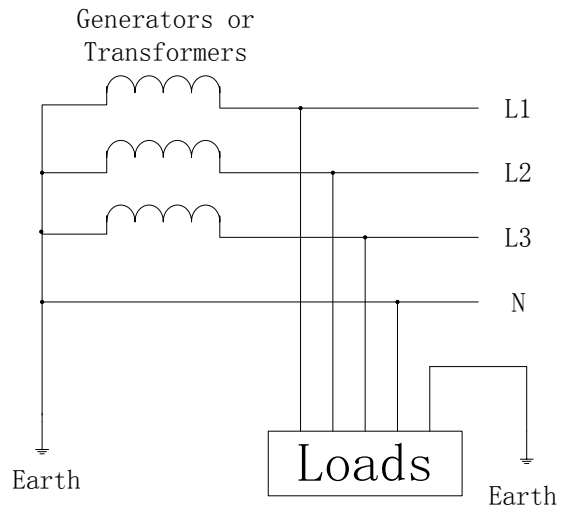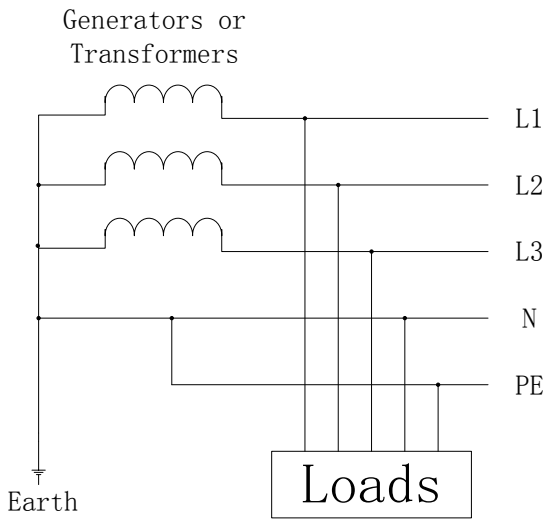
Figure 1.3 TN-C-S grounding system [16]   Figure 1.4 TT grounding system [16]

Generators or
Transformers

L1

L2

L3

Loads

Earth

Figure 1.5 IT grounding system [16]

1.3 The Distributed Generation and the Micro-grid's Influence on the Large Grid

A few number of distributed sources have little influence on the large grid.

However, if there are many distributed generation units or some large capacity generation

9

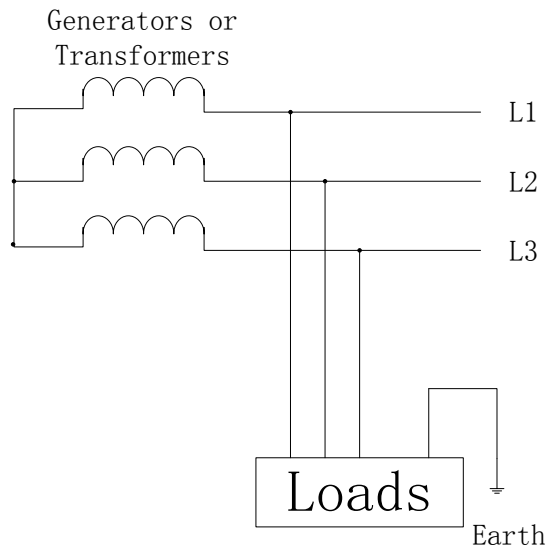units interconnected with the main grid, the performance of the large grid will be influenced seriously. The negative effects may include issues with transient stability, dynamic stability, voltage stability, frequency stability, voltage waveform, voltage flicker, harmonic, short circuit current, and active/reactive power flow [17]. Specifically, the influence can decrease the system stability and the power quality. In this way, the system cannot operate safely and reliably.

1.3.1   Stability Analysis

When the micro-grid and the external grid are in parallel operation mode, the micro-grid will have influence on the external grid stability. When disconnecting the micro-grid from the external grid, the micro-grid needs smoothly transit from the grid-connected operation mode to the islanded operation mode. The system stability problem during this process needs to be studied.

There are two methods to analyze the stability of the distribution system with multiple distributed generation units [18]. One is based on the complex dynamic model. It adopts Prony algorithm, and defines the signal residue as the criterion of the system stability. The other one is observing the change of the system stability limit with different parameters. It defines the system stability limit as the criterion of the system stability. Analysis indicates that the power electronic interfaced distributed generation unit plays a negative role in the system stability, but its voltage control and the loads of certain type

10

of distributed sources play a positive role in the system stability. Distributed sources and grid-connected micro-grids will impact the distribution system voltage control due to the following four reasons. The first one is the present automatic voltage controllers are used to control the voltage amplitude of the passive distribution system. The second one is that distributed generation systems are usually far from the main substation. It is difficult to control the voltage in the main substation. If the lines between the substation and generators have large resistance and low load density, the voltage control can probably fail. The third one is that if the capacity of the distributed sources connected by a feeder line is larger than that of the whole feeder circuit, the direction of the flow through the transformer will reverse, and the low voltage side of the step-down transformer will become the source. The last one is that the type of the distributed generation devices (synchronous machines, asynchronous machines, power electronic equipment, etc.) and the operation conditions influence the voltage control [19].

The main factors that affect the micro-grid stability consist of the control strategy of micro-sources and energy storage systems, types of loads, fault locations, and inertia constant of generators. During the normal operation mode, the control device of the micro-grid can use local information to control micro-sources and energy storage devices, and the control strategies contain P-Q control, droop control and frequency/voltage control [20]. Simulation study indicates that constant P-Q loads and resistive loads have little influence on the micro-grid with flywheel energy storage systems, and that the

motor with large inertia constant can enhance the micro-grid stability. The most remarkable influence to the micro-grid is the faults of the large grid.

1.3.2 Power Quality

After the distributed generation or the micro-grid is connected with the distribution system, voltage flicker and harmonic will appear if without proper controlling. On the other hand, the grid-connected distributed generation or micro-grid can also improve the power quality by converter technologies [21]. Furthermore, harmonic control and reactive control can be realized by power electronic technologies. When the micro-grid runs in the islanded operation mode, the power quality can be improved by flexible AC transmission system (FACTS) technologies and energy storage technologies.

The different fault levels, ratios of resistance/reactance, types of distributed generators and prime movers of the grid have different influences on the grid voltage stability, flicker, waveform distortion, and unbalance.

1.3.3 Planning and Operation

Distributed sources and micro-grids, installed locations, installed capacity, and penetration limits of different types of distributed generation systems must be taken into

consideration besides loads demand, economics, security, reliability, and power loss [22]. Therefore, the optimization of system operation is important. The optimization of installed locations of distributed generation systems or micro-grids should consider the capacity limit, voltage waveform of feeder lines, and the current level of three phase short circuit. According to them, the objective function and the constraints can be set. Various algorithms can be used to determine the locations and capacity of distributed generation units; e.g., the genetic algorithm.

1.3.4   Power Loss

Power loss depends on system power flow [23]. The grid-connected distributed sources and micro-grids make the power flow no longer one-way, which inevitably influences the power loss. The power loss is not only related to loads, but also is related to locations of grid-connected distributed resource units, relative values of capacity and loads, and network topologies. The analysis of the normal operation mode of the induction machines in the distribution system indicates that if the installed location of an induction machine is farther from the substation, the induction machine will have larger influences on the power loss. The capacity and installed location of generation systems can influence the transmission parameters, which leads to different voltage drops.

Chapter 2: System Identification

System identification is used to determine a system from a class of systems that is equivalent to the observed system with output response to known input [24]. It can be classified and analyzed based on different methods.

System identification can be divided into linear system identification, nonlinear system identification [25,26], lumped parameter system identification and distributed parameter system identification by mathematic models adopted for the research [27], system structure identification and system parameter identification by known system information [28], open-loop identification and close-loop identification by system structures [29], or on-line identification and off-line identification by methods used for parameter estimation [30].

The system structure identification problem is also called the complete identification problem [31]. It supposes that the studied system is completely unknown. It is necessary to firstly identify the model of the system, and then identify the parameters of the system model, which is similar to a black-box problem. There are many methods

which can be used in this research area [24,32], e.g., polynomials, Volterra series, Wiener series, the force state chart, Hilbert transformation, complex stiffness, etc.

The system parameter identification problem is also called the partial identification problem. It is supposed that both the system structure and the mathematic model of the studied system are known in advance. The parameters of the system model need to be identified, which is similar to the grey-box problem. Many approaches can be adopted in this identification problem; e.g., time domain, frequency domain, NARMAX model, NLAR model, NLARMA model, NLARMAV model, etc.

The partial identification problem indicates that after obtaining the mathematic model, undetermined parameters of the model need to be estimated by experiment data. This is a parameter estimation problem, which consists of parameter estimation principle and parameter estimation algorithm. The principle is used to judge whether the calculated parameters satisfy the requirements of the identification. The common principles used are least squares, maximum likelihood, minimum variance, minimum risk, etc. The algorithm can be divided into iterative algorithm and recursive algorithm. The iterative algorithm includes Newton method, gradient method, and Gaussian method, whereas the recursive algorithm includes real-time on-line estimation, point-by-point data processing, and parameter updating [33].

The least squares method was proposed by Gauss when he studied planets motion trajectory [34]. And then the least squares method became the foundation of the estimation theory. The minimum square sum of error is adopted for the principle of the least squares method, in order to obtain the optimized parameters that ensure the matching of experimental data. The method has many expanding forms such as recursive least squares method, generalized least squares method, multi-level least squares method and instrumental variable method.

The maximum likelihood method is proposed by the famous statistician Fischer [35]. The maximum likelihood estimation method establishes the probabilistic characteristic and statistical relationship between random observed data and unknown parameters by introducing the likelihood function of the relative random variables. The factor distributed density function is called the likelihood function. The method maximizes the likelihood function by estimation of the unknown parameters.

Several issues are involved in the closed-loop system identification research; e.g., the detection of feedback loop, conditions of closed-loop identification, methods of closed-loop identification, the utilization of the open-loop identification in the closed-loop identification problem. Many methods can be adopted for judging whether the feedback loop exists in the system or not, e.g., spectral factorization method, likelihood ratio test method, etc. Whether the system can be identified or not is the condition of

16

closed-loop identification. The method of closed-loop identification includes indirect identification and direct identification.

The conventional approaches of transfer function identification include time domain method and frequency domain method. The time domain method includes step response method, impulse response method, and rectangular pulse response method, among which the step response method has attracted great attention and has been widely used recently. The step response method uses the system step response curve to identify the system transfer function.

Chapter 3: Method and Algorithm

3.1 Least Squares Method

The least squares method is a mathematic optimization technology. It was firstly proposed by Gauss and published in his book *Theoria Motus Corporum Coelestium in Sectionibus Conicis Solem Ambientium* in 1809. Simply said, the method is to make the sum of squares of the differences between estimated values and true values less and less until the difference is little enough to indicate the estimated values can be adopted. This method can be used in many problems.

3.1.1   Estimation of a Constant

Suppose there is an unknown parameter. The purpose is to estimate the value of it with some measurements containing noise. Assume that $\mathbf{x} = (x_1, x_2, \dots, x_n)^T$ is an unknown constant vector, and $\mathbf{y} = (y_1, y_2, \dots, y_k)^T$ is a k-element noisy measurement vector. To find the best estimate, the simplest case can be considered in which each $\mathbf{y}$ is a linear combination of $\mathbf{x}$, with addition of some measurement noise $\mathbf{v}$. Thus:

$$\mathbf{y} = \mathbf{Hx} + \mathbf{v} \qquad (3\text{-}1)$$

where, $\mathbf{v} = (v_1, v_2, \dots, v_k)^T$, and $\mathbf{H}$ is a $k \times n$ matrix. So the equation (3-1) can be re-written as follows.

$$\begin{pmatrix} y_1 \\ \vdots \\ y_k \end{pmatrix} = \begin{pmatrix} H_{11} & \cdots & H_{1n} \\ \vdots & \ddots & \vdots \\ H_{k1} & \cdots & H_{kn} \end{pmatrix} \begin{pmatrix} x_1 \\ \vdots \\ x_n \end{pmatrix} + \begin{pmatrix} v_1 \\ \vdots \\ v_k \end{pmatrix} \qquad (3\text{-}2)$$

Given an estimate $\hat{x}$, the difference between the noisy measurements and the expected values is:

$$\boldsymbol{\varepsilon} = \mathbf{y} - \mathbf{H\hat{x}} \qquad (3\text{-}3)$$

Under the least squares principle, we will try to find the value of $\mathbf{\hat{x}}$ that minimizes the cost function:

$$\mathbf{J(\hat{x})} = \boldsymbol{\varepsilon}^\mathbf{T}\boldsymbol{\varepsilon} = (\mathbf{y} - \mathbf{H\hat{x}})^\mathbf{T}(\mathbf{y} - \mathbf{H\hat{x}}) = \mathbf{y}^\mathbf{T}\mathbf{y} - \mathbf{\hat{x}}^\mathbf{T}\mathbf{H}^\mathbf{T}\mathbf{y} - \mathbf{y}^\mathbf{T}\mathbf{H\hat{x}} + \mathbf{\hat{x}}^\mathbf{T}\mathbf{H}^\mathbf{T}\mathbf{H\hat{x}} \qquad (3\text{-}4)$$

The necessary condition for the minimum is that the partial derivative (gradient) of $\mathbf{J}$ with respect to $\mathbf{\hat{x}}$ equals to zero.

$$\frac{\partial \mathbf{J}}{\partial \mathbf{\hat{x}}} = -\mathbf{2y}^\mathbf{T}\mathbf{H} + \mathbf{2\hat{x}}^\mathbf{T}\mathbf{H}^\mathbf{T}\mathbf{H} = \mathbf{0}$$

$$(3\text{-}5)$$

Then we get:

$$\mathbf{\hat{x}} = (\mathbf{H}^\mathbf{T}\mathbf{H})^{-\mathbf{1}}\mathbf{H}^\mathbf{T}\mathbf{y} \qquad (3\text{-}6)$$

The inverse $(\mathbf{H}^\mathbf{T}\mathbf{H})^{-\mathbf{1}}$ exists if $k > n$ and $\mathbf{H}$ is non-singular [34].

3.1.2 Weighed Least Squares Estimation

Suppose that confidence is not equal on all measurements. For example, some of parameters are measured with low noise, whereas the others are measured with large noise. The other factors are the same as the ones described in section 3.1.1, so the process can also start with the function (3-1). Assume that each measurement may be taken under different conditions so that the variance of the measurement noise may be distinct too:

$$E(v_i^2) = \sigma_i^2, \qquad 1 \leq i \leq k \tag{3-7}$$

Assume that the noise for each measurement has zero mean and is independent [36]. The covariance matrix for all measurement noise is:

$$R = E(vv^T) = \begin{pmatrix} \sigma_1^2 & \cdots & 0 \\ \vdots & \ddots & \vdots \\ 0 & \cdots & \sigma_k^2 \end{pmatrix} \tag{3-8}$$

Via the function (3-3), the sum of squared differences weighted over the variance of the measurements can be minimized.

$$J(\hat{x}) = \varepsilon^T R^{-1} \varepsilon = \frac{\varepsilon_1^2}{\sigma_1^2} + \frac{\varepsilon_2^2}{\sigma_2^2} + \cdots + \frac{\varepsilon_k^2}{\sigma_k^2} = 0$$

$$\tag{3-9}$$

Then the equation (3-9) can be expanded as:

$$J(\hat{x}) = \varepsilon^T R^{-1} \varepsilon = (y - H\hat{x})^T R^{-1} (y - H\hat{x})$$

$$= y^T R^{-1} y - \hat{x}^T H^T R^{-1} y - y^T R^{-1} H\hat{x} + \hat{x}^T H^T R^{-1} H\hat{x} = 0 \tag{3-10}$$

Therefore, the estimation result is:

$$\hat{x} = (H^T R^{-1} H)^{-1} H^T R^{-1} y \tag{3-11}$$

3.1.3 Recursive Least Squares Estimation

If measurements are obtained sequentially and estimates need to be updated by each new measurement [37], the matrix $\mathbf{H}$ needs to be augmented as well. The vector $\hat{\mathbf{x}}$ has to be re-computed when updating. That will involve very large computations. Suppose there is an estimate $\hat{\mathbf{x}}_{k-1}$ after $k-1$ updating, then the purpose is to update the estimate by $\hat{\mathbf{x}}_k$ without having to solve $\hat{\mathbf{x}} = (\mathbf{H}^T\mathbf{R}^{-1}\mathbf{H})^{-1}\mathbf{H}^T\mathbf{R}^{-1}\mathbf{y}$. A linear recursive estimator can be written as [37]:

$$\mathbf{y}_k = \mathbf{H}_k\mathbf{x} + \mathbf{v}_k \tag{3-12}$$

$$\hat{\mathbf{x}}_k = \hat{\mathbf{x}}_{k-1} + \mathbf{K}_k(\mathbf{y}_k - \mathbf{H}_k\hat{\mathbf{x}}_{k-1}) \tag{3-13}$$

where, $\mathbf{H}_k$ is a row vector, and $\mathbf{K}_k$ is a $n \times k$ matrix referred to as the estimator gain matrix. $(\mathbf{y}_k - \mathbf{H}_k\hat{\mathbf{x}}_{k-1})$ is referred to as the correction term. The new estimate $\hat{\mathbf{x}}_k$ is modified from the previous estimate $\hat{\mathbf{x}}_{k-1}$ by a correction gain matrix and a correction term. The current estimation error is $\boldsymbol{\varepsilon}_k = \mathbf{x} - \hat{\mathbf{x}}_k$. The mean of this error is computed:

$$\mathbf{E}(\boldsymbol{\varepsilon}_k) = \mathbf{E}(\mathbf{x} - \hat{\mathbf{x}}_k) = \mathbf{E}\big(\mathbf{x} - \hat{\mathbf{x}}_{k-1} - \mathbf{K}_k(\mathbf{y}_k - \mathbf{H}_k\hat{\mathbf{x}}_{k-1})\big)$$

$$= \mathbf{E}\big(\boldsymbol{\varepsilon}_{k-1} - \mathbf{K}_k(\mathbf{H}_k\mathbf{x} + \mathbf{v}_k - \mathbf{H}_k\hat{\mathbf{x}}_{k-1})\big)$$

$$= \mathbf{E}(\boldsymbol{\varepsilon}_{k-1} - \mathbf{K}_k\mathbf{H}_k(\mathbf{x} - \hat{\mathbf{x}}_{k-1}) - \mathbf{K}_k\mathbf{v}_k)$$

$$= (\mathbf{I} - \mathbf{K}_k\mathbf{H}_k)\mathbf{E}(\boldsymbol{\varepsilon}_{k-1}) - \mathbf{K}_k\mathbf{E}(\mathbf{v}_k) \tag{3-14}$$

where $\mathbf{I}$ is the $n \times n$ identity matrix. If $\mathbf{E}(\mathbf{v}_k) = 0$ and $\mathbf{E}(\boldsymbol{\varepsilon}_{k-1}) = 0$, then $\mathbf{E}(\boldsymbol{\varepsilon}_k) = 0$. So if the measurement noise v_k has zero mean for all k, and the initial estimate of x is set equal to its expected value, then $\hat{x}_k = x_k$ for all k. With this property, the estimator

21

$(\widehat{x}_k = \widehat{x}_{k-1} - K_k(y_k - H_k\widehat{x}_{k-1}))$ is called unbiased. The property holds regardless of the value of the gain matrix $\mathbf{K_k}$. It says that on the average the estimate $\widehat{\mathbf{x}}$ will be equal to the true value $\mathbf{x}$. The key problem is to determine the optimal value of the gain matrix $\mathbf{K_k}$. The optimality criterion used is to minimize the aggregated variance of the estimation errors at time k:

$$\mathbf{J_k} = \mathbf{E}(\|\mathbf{x} - \widehat{\mathbf{x}}_k\|^2) = \mathbf{E}(\boldsymbol{\varepsilon_k}^T\boldsymbol{\varepsilon_k}) = \mathbf{E}\left(\mathbf{tr}(\boldsymbol{\varepsilon_k}\boldsymbol{\varepsilon_k}^T)\right) = \mathbf{tr}(\mathbf{P_k}) \qquad (3\text{-}15)$$

where, tr is the trace operator, and $(\mathbf{P_k} = \mathbf{E}(\boldsymbol{\varepsilon_k}\boldsymbol{\varepsilon_k}^T))$ is the estimation-error covariance. Next, $\mathbf{P_k}$ can be obtained by the equation given as follows.

$$\mathbf{P_k} = \mathbf{E}\big(((\mathbf{I} - \mathbf{K_k}\mathbf{H_k})\mathbf{E}(\boldsymbol{\varepsilon_k}) - \mathbf{K_k}\mathbf{v_k})((\mathbf{I} - \mathbf{K_k}\mathbf{H_k})\mathbf{E}(\boldsymbol{\varepsilon_{k-1}}) - \mathbf{K_k}\mathbf{v_k})^T\big)$$

$$= (\mathbf{I} - \mathbf{K_k}\mathbf{H_k})\mathbf{E}(\boldsymbol{\varepsilon_{k-1}}\boldsymbol{\varepsilon_{k-1}}^T)(\mathbf{I} - \mathbf{K_k}\mathbf{H_k})^T - \mathbf{K_k}\mathbf{E}(\mathbf{v_k}\boldsymbol{\varepsilon_{k-1}}^T)(\mathbf{I} - \mathbf{K_k}\mathbf{H_k})^T$$

$$- (\mathbf{I} - \mathbf{K_k}\mathbf{H_k})\mathbf{E}(\boldsymbol{\varepsilon_{k-1}}\mathbf{v_k}^T)\mathbf{K_k}^T + \mathbf{K_k}\mathbf{E}(\mathbf{v_k}\mathbf{v_k}^T)\mathbf{K_k}^T$$

$$= (\mathbf{I} - \mathbf{K_k}\mathbf{H_k})\mathbf{P_{k-1}}(\mathbf{I} - \mathbf{K_k}\mathbf{H_k})^T + \mathbf{K_k}\mathbf{R_k}\mathbf{K_k}^T \qquad (3\text{-}16)$$

where $(\mathbf{R_k} = \mathbf{E}(\mathbf{v_k}\mathbf{v_k}^T))$ is the covariance of $\mathbf{v_k}$. The estimation error $\boldsymbol{\varepsilon_{k-1}}$ at time $k-1$ is independent with respect to the measurement noise v_k at time k. The latter implies that:

$$\mathbf{E}(\mathbf{v_k}\boldsymbol{\varepsilon_{k-1}}^T) = \mathbf{E}(\mathbf{v_k})\mathbf{E}(\boldsymbol{\varepsilon_{k-1}}) = \mathbf{0} \qquad (3\text{-}17)$$

Then, the value of the gain matrix K_k will be found by minimizing the cost function.

$$\frac{\partial \mathbf{J_k}}{\partial \mathbf{K_k}} = 2(\mathbf{I} - \mathbf{K_k}\mathbf{H_k})\mathbf{P_{k-1}}(-\mathbf{H_k}^T) + 2\mathbf{K_k}\mathbf{R_k} = \mathbf{0}$$

$$(3\text{-}18)$$

Finally, the gain matrix K_k can be obtained.

$$\mathbf{K_k} = \mathbf{P_{k-1}}\mathbf{H_k}^T(\mathbf{H_k}\mathbf{P_{k-1}}\mathbf{H_k}^T + \mathbf{R_k})^{-1} \qquad (3\text{-}19)$$

22

3.2 Newton-Raphson Algorithm

Newton-Raphson algorithm is used to find the roots of a system of equations [38, 39]. Assume there is an equation to be solved as follows:

$$f(x) = 0 \tag{3-20}$$

First select an initial value $x^{(0)}$ which is close to zero point. Then draw the tangent line through the point $(x^{(0)}, f(x^{(0)}))$ and calculate the intersection point between the tangent line and x-axis. This point can be called $(x^{(1)}, 0)$.

$$x^{(1)} = x^{(0)} - \frac{f(x^{(0)})}{f'(x^{(0)})}$$

$$\tag{3-21}$$

$x^{(1)}$ should be more close to the zero point than $x^{(0)}$. Finally, after n times of iteration, the roots can be obtained.

$$x^{(n)} = x^{(n-1)} - \frac{f(x^{(n-1)})}{f'(x^{(n-1)})}$$

$$\tag{3-22}$$

So when solving a system of equations, the principle is the same. Assume there is a system of equations.

$$\mathbf{f}(\mathbf{x}) = \mathbf{0} \tag{3-23}$$

The system of equations has m equations and m unknown variables. So the equation can also be written as another form.

$$\begin{cases} f_1(x_1, x_2 \dots x_m) = 0 \\ \qquad \dots \\ f_m(x_1, x_2 \dots x_m) = 0 \end{cases} \qquad (3\text{-}24)$$

The roots of the system of equations are as follows.

$$\mathbf{x}^{(n)} = \mathbf{x}^{(n-1)} - \mathbf{J}^{-1}\mathbf{f}(\mathbf{x}^{(n-1)}) \qquad (3\text{-}25)$$

$$\mathbf{x}^{(n)} = (x_1^{(n)}, x_2^{(n)} \dots x_m^{(n)})^{\mathbf{T}} \qquad (3\text{-}26)$$

$$\mathbf{x}^{(n-1)} = (x_1^{(n-1)}, x_2^{(n-1)} \dots x_m^{(n-1)})^{\mathbf{T}} \qquad (3\text{-}27)$$

$$\mathbf{J} = \begin{pmatrix} \dfrac{\partial f_1(\mathbf{x}^{(n-1)})}{\partial x_1^{(n-1)}} & \dots & \dfrac{\partial f_1(\mathbf{x}^{(n-1)})}{\partial x_m^{(n-1)}} \\ \vdots & \ddots & \vdots \\ \dfrac{\partial f_m(\mathbf{x}^{(n-1)})}{\partial x_1^{(n-1)}} & \dots & \dfrac{\partial f_m(\mathbf{x}^{(n-1)})}{\partial x_m^{(n-1)}} \end{pmatrix}$$

$$(3\text{-}28)$$

3.3 The Process of Parameter Identification

The process of parameter identification based on the least squares method and Newton-Raphson algorithm is shown as follows.
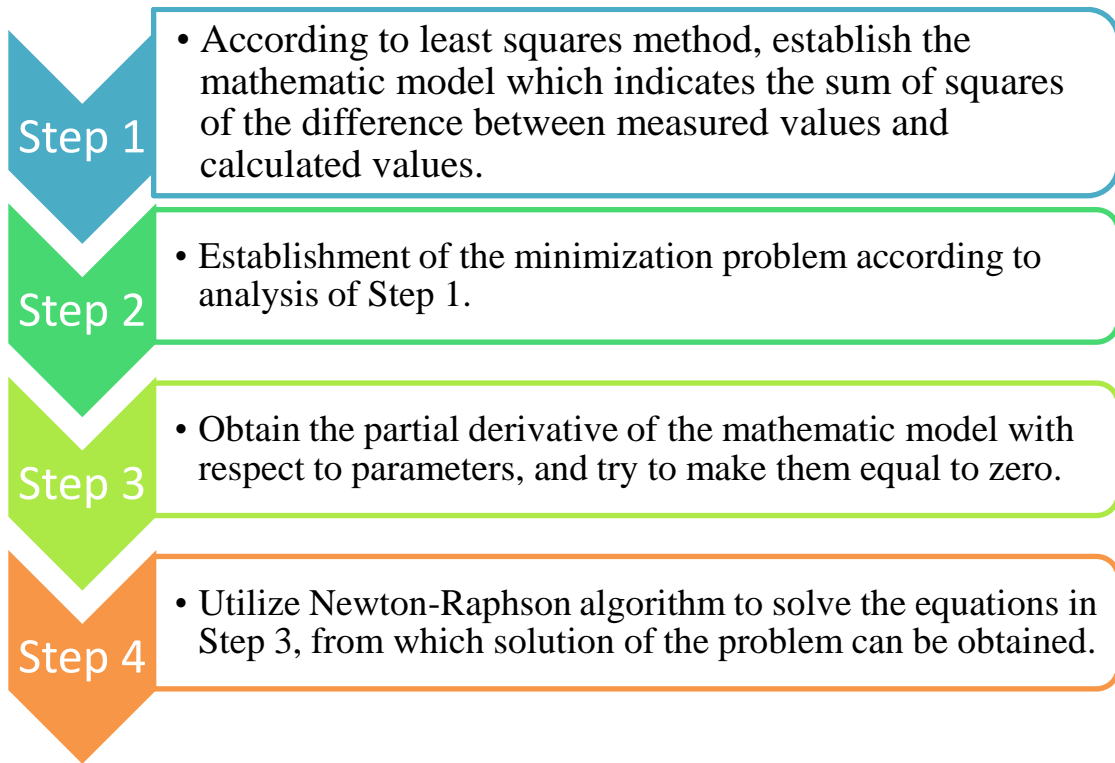
Step 1 • According to least squares method, establish the mathematic model which indicates the sum of squares of the difference between measured values and calculated values.

Step 2 • Establishment of the minimization problem according to analysis of Step 1.

Step 3 • Obtain the partial derivative of the mathematic model with respect to parameters, and try to make them equal to zero.

Step 4 • Utilize Newton-Raphson algorithm to solve the equations in Step 3, from which solution of the problem can be obtained.

Figure 3.1 The basic process of identification

Fig. 3.1 indicates the basic process of parameter identification including the following four steps.

Step 1: Assume there is a system $f(s)$, with u as its input signal and y as the relative output signal. Therefore, the function can be expressed as follows.

$$y = uf(s) \tag{3-29}$$

Assume that the system has j unknown parameters.

$$\mathbf{K} = \left(K_1, K_2 \dots K_j \right)^T \tag{3-30}$$

The input signal u is known, and n sample values of $\mathbf{f}$ at time $\mathbf{t}$ are obtained by measurements.

25

$$\mathbf{f} = (f_1, f_2 \ldots f_n)^T \tag{3-31}$$

$$\mathbf{t} = (t_1, t_2 \ldots t_n)^T \tag{3-32}$$

Here the sample points $\mathbf{f}$ can be called criterion sample points for convenience. The final

purpose is to determine the value of parameter $\widehat{\mathbf{K}}$ which is very close to the true value of

the parameter K.

$$\widehat{\mathbf{K}} = \left(\widehat{K}_1, \widehat{K}_2 \ldots \widehat{K}_j\right)^T \tag{3-33}$$

Firstly, $\widehat{\mathbf{K}}$ can be set as an initial value $\widehat{\mathbf{K}}^{(0)}$, so the initial values can be shown as:

$$\widehat{\mathbf{K}}^{(0)} = (\widehat{K}_1^{(0)}, \widehat{K}_2^{(0)} \ldots \widehat{K}_j^{(0)})^T \tag{3-34}$$

Then the initial function can be transferred from the frequency-domain form to the time-

domain form, that is:

$$y = uf(t) \tag{3-35}$$

In function (3-35), if the parameters $\mathbf{K}$ are set equal to $\widehat{\mathbf{K}}^{(0)}$, we can get a y-t curve. Then

n sample points $\mathbf{f}_\mathbf{p}^{(0)}$ can also be obtained from the curve at time t.

$$\mathbf{f}_\mathbf{p}^{(0)} = (f_{p1}^{(0)}, f_{p2}^{(0)} \ldots f_{pn}^{(0)})^T \tag{3-36}$$

The sample points $\mathbf{f}_\mathbf{p}^{(0)}$ are certainly different from the sample points $\mathbf{f}$, because

$\widehat{\mathbf{K}}^{(0)}$ is generally certainly different from $\widehat{\mathbf{K}}$, or else there is no need to do the parameter

identification. So in the end, the value $\widehat{\mathbf{K}}$ finally makes the y-t curve match the sample

points $\mathbf{f}$. Here the least squares method and Newton-Raphson algorithm can be adopted

for the identification of the parameter vector $\widehat{\mathbf{K}}$.

The least squares method is used to judge whether the value of the parameter reaches the requirement or not. If the value of the parameter does not reach the requirement, Newton-Raphson algorithm will be used to update the value of the parameter. The process is as follows. First, n sample points $\mathbf{f_p}^{(0)}$ are obtained by the initial value $\widehat{\mathbf{K}}^{(0)}$ as mentioned. Then we can get the differences between $\mathbf{f_p}^{(0)}$ and $\mathbf{f}$.

$$\mathbf{f_p}^{(0)} - \mathbf{f} = (f_{p1}^{(0)} - f_1, f_{p2}^{(0)} - f_2 \cdots f_{pn}^{(0)} - f_{1n})^T \tag{3-37}$$

From (3-37), the sum of squares of these differences is given as follows.

$$\sum_{i=1}^{n} (f_{pi}^{(0)} - f_i)^2 \tag{3-38}$$

In the function, f_i is the criterion sample point at time t_i, and $f_{pi}^{(0)}$ is the sample point at time t_i when the parameters are $\widehat{\mathbf{K}}^{(0)}$. t_i is an element of $\mathbf{t}$. Here a small enough value ε should be set, and if (3-38) is larger than ε, it indicates that $\widehat{\mathbf{K}}^{(0)}$ are far from the true values of the system. Therefore, the parameters $\widehat{\mathbf{K}}^{(0)}$ need to be optimized, the parameters after updating can be called $\widehat{\mathbf{K}}^{(1)}$.

$$\widehat{\mathbf{K}}^{(1)} = (\widehat{K}_1^{(1)}, \widehat{K}_2^{(1)} \cdots \widehat{K}_j^{(1)})^T \tag{3-39}$$

$$\Delta\mathbf{K}^{(1)} = \widehat{\mathbf{K}}^{(1)} - \widehat{\mathbf{K}}^{(0)} = (\widehat{K}_1^{(1)} - \widehat{K}_1^{(0)}, \widehat{K}_2^{(1)} - \widehat{K}_2^{(0)} \cdots \widehat{K}_j^{(1)} - \widehat{K}_j^{(0)})^T$$

$$= (\Delta K_1^{(1)}, \Delta K_2^{(1)} \cdots \Delta K_j^{(1)})^T \tag{3-40}$$

To get $\Delta\mathbf{K}^{(1)}$, Newton-Raphson algorithm can be used. The function of the squares of the difference between f_i and the y-t curve at time t_i is as follows.

$$F_i = (y_{Ki} - f_i)^2 \tag{3-41}$$

In this function, y_{Ki} is the function with respect to $\mathbf{K}$ at time t_i, and the structure of the function is the same as y.

$$y_{Ki} = uf(\mathbf{K}) \tag{3-42}$$

Step 2: The final objective is to make (3-38) as small as possible, so when updating $\mathbf{K}$, function (3-41) should be minimized. There are many methods to obtain the minimum of function F_i, e.g., gradient method, Gaussian method, etc.

Step 3: In order to compute the minimization problem, we minimize the function by making its partial derivative with respect to $\mathbf{K}$ equal to zero.

$$\mathbf{F_i'} = \frac{\partial F_i}{\partial \mathbf{K}} = \frac{\partial (y_{Ki} - f_i)^2}{\partial \mathbf{K}} = 2(y_{Ki} - f_i)\frac{\partial y_{Ki}}{\partial \mathbf{K}} = 0$$

$$\tag{3-43}$$

Therefore, the equation (3-43) can also be written in matrix form.

$$\mathbf{F_i'} = \begin{pmatrix} F_{i1}' \\ \vdots \\ F_{ij}' \end{pmatrix} = 2(y_{Ki} - f_i)\begin{pmatrix} \frac{\partial y_{Ki}}{\partial K_1} \\ \vdots \\ \frac{\partial y_{Ki}}{\partial K_j} \end{pmatrix} = 0 \tag{3-44}$$

Step 4: Newton-Raphson algorithm is adopted to find the root of (3-44), where Taylor series expansion method need to be used. $\widehat{\mathbf{K}}^{(0)}$ are set as the initial values. Then, Taylor series are expanded at the initial point $(\widehat{\mathbf{K}}^{(0)}, F_i'(\widehat{\mathbf{K}}^{(0)}))$, with only the linear part reserved.

$$\mathbf{F_i'} = \mathbf{F_i'}(\widehat{\mathbf{K}}^{(0)}) + \left.\frac{\partial \mathbf{F_i'}}{\partial \mathbf{K}}\right|_{\mathbf{K}=\widehat{\mathbf{K}}^{(0)}} \left(\mathbf{K} - \widehat{\mathbf{K}}^{(0)}\right) + \left.\frac{\partial^2 \mathbf{F_i'}}{\partial \mathbf{K}^2}\right|_{\mathbf{K}=\widehat{\mathbf{K}}^{(0)}} \left(\mathbf{K} - \widehat{\mathbf{K}}^{(0)}\right)^2 + \cdots$$

$$\approx \mathbf{F_i'}(\widehat{\mathbf{K}}^{(0)}) + \left.\frac{\partial \mathbf{F'}}{\partial \mathbf{K}}\right|_{\mathbf{K}=\widehat{\mathbf{K}}^{(0)}} \left(\mathbf{K} - \widehat{\mathbf{K}}^{(0)}\right)$$

Based on (3-43) and (3-45), the following equation can be obtained.

$$\mathbf{F_i'}\left(\widehat{\mathbf{K}}^{(0)}\right) + \left.\frac{\partial \mathbf{F_i'}}{\partial \mathbf{K}}\right|_{\mathbf{K}=\widehat{\mathbf{K}}^{(0)}} \left(\mathbf{K} - \widehat{\mathbf{K}}^{(0)}\right) = \mathbf{0}$$

The equation can be also written in the following matrix form.

$$\begin{pmatrix} F_{i1}' \\ \vdots \\ F_{ij}' \end{pmatrix} + \begin{pmatrix} \dfrac{\partial F_{i1}'}{\partial \widehat{K}_1^{(0)}} & \cdots & \dfrac{\partial F_{i1}'}{\partial \widehat{K}_j^{(0)}} \\ \vdots & \ddots & \vdots \\ \dfrac{\partial F_{ij}'}{\partial \widehat{K}_1^{(0)}} & \cdots & \dfrac{\partial F_{ij}'}{\partial \widehat{K}_j^{(0)}} \end{pmatrix} \begin{pmatrix} K_1 - \widehat{K}_1^{(0)} \\ \vdots \\ K_j - \widehat{K}_j^{(0)} \end{pmatrix} = 0$$

In this way, the root of equation (3-47) can be obtained.

$$\begin{pmatrix} \widehat{K}_1^{(1)} \\ \vdots \\ \widehat{K}_j^{(1)} \end{pmatrix} = \begin{pmatrix} \widehat{K}_1^{(0)} \\ \vdots \\ \widehat{K}_j^{(0)} \end{pmatrix} - \begin{pmatrix} \dfrac{\partial F_{i1}'}{\partial \widehat{K}_1^{(0)}} & \cdots & \dfrac{\partial F_{i1}'}{\partial \widehat{K}_j^{(0)}} \\ \vdots & \ddots & \vdots \\ \dfrac{\partial F_{ij}'}{\partial \widehat{K}_1^{(0)}} & \cdots & \dfrac{\partial F_{ij}'}{\partial \widehat{K}_j^{(0)}} \end{pmatrix}^{-1} \begin{pmatrix} F_{i1}' \\ \vdots \\ F_{ij}' \end{pmatrix}$$

$$\begin{pmatrix} \Delta K_1^{(1)} \\ \vdots \\ \Delta K_j^{(1)} \end{pmatrix} = - \begin{pmatrix} \dfrac{\partial F_{i1}'}{\partial \widehat{K}_1^{(0)}} & \cdots & \dfrac{\partial F_{i1}'}{\partial \widehat{K}_j^{(0)}} \\ \vdots & \ddots & \vdots \\ \dfrac{\partial F_{ij}'}{\partial \widehat{K}_1^{(0)}} & \cdots & \dfrac{\partial F_{ij}'}{\partial \widehat{K}_j^{(0)}} \end{pmatrix}^{-1} \begin{pmatrix} F_{i1}' \\ \vdots \\ F_{ij}' \end{pmatrix}$$

when $\begin{pmatrix} \dfrac{\partial F_{i1}'}{\partial \widehat{K}_1^{(0)}} & \cdots & \dfrac{\partial F_{i1}'}{\partial \widehat{K}_j^{(0)}} \\ \vdots & \ddots & \vdots \\ \dfrac{\partial F_{ij}'}{\partial \widehat{K}_1^{(0)}} & \cdots & \dfrac{\partial F_{ij}'}{\partial \widehat{K}_j^{(0)}} \end{pmatrix} \neq 0.$

The parameters $\widehat{K}$ in the system can be updated by this method until $\sum_{i=1}^{n}(f_{pi}^{(q)} - f_i)^2$ is smaller than ε. If we get the result after q times of iteration, the last equation will be:

$$\begin{pmatrix} \widehat{K}_1^{(q)} \\ \vdots \\ \widehat{K}_j^{(q)} \end{pmatrix} = \begin{pmatrix} \widehat{K}_1^{(q-1)} \\ \vdots \\ \widehat{K}_j^{(q-1)} \end{pmatrix} - \begin{pmatrix} \dfrac{\partial F_{i1}'}{\partial \widehat{K}_1^{(q-1)}} & \cdots & \dfrac{\partial F_{i1}'}{\partial \widehat{K}_j^{(q-1)}} \\ \vdots & \ddots & \vdots \\ \dfrac{\partial F_{ij}'}{\partial \widehat{K}_1^{(q-1)}} & \cdots & \dfrac{\partial F_{ij}'}{\partial \widehat{K}_j^{(q-1)}} \end{pmatrix}^{-1} \begin{pmatrix} F_{i1}' \\ \vdots \\ F_{ij}' \end{pmatrix}$$

(3-50)

when $\begin{pmatrix} \dfrac{\partial F_{i1}'}{\partial \widehat{K}_1^{(q-1)}} & \cdots & \dfrac{\partial F_{i1}'}{\partial \widehat{K}_j^{(q-1)}} \\ \vdots & \ddots & \vdots \\ \dfrac{\partial F_{ij}'}{\partial \widehat{K}_1^{(q-1)}} & \cdots & \dfrac{\partial F_{ij}'}{\partial \widehat{K}_j^{(q-1)}} \end{pmatrix} \neq 0.$

Chapter 4: Results

4.1 The Functions and Types of Microgrid Controls

A micro-grid system generally has two operation modes, i.e., grid-connected

operation mode and islanded mode. The control of the micro-grid plays an important role

both in grid-connected operation mode and in islanded mode. In the grid-connected

operation mode, the micro-grid system should be treated as a constant load or a constant

generator. The control system of the micro-grid is to determine how much power the

micro-grid should consume or generate [40, 41]. Whereas, in the islanded operation mode,

the condition of the micro-grid is different from the one of the other operation mode.

Unlike the conventional large grid, the micro-grid does not have enough inertia. It makes

the micro-grid far more flexible than the conventional large grid, but it also decreases the

anti-disturbance ability of the micro-grid. So the control system is critical to the stability

of the micro-grid. A typical dual-loop control system for microgrid inverter is shown in
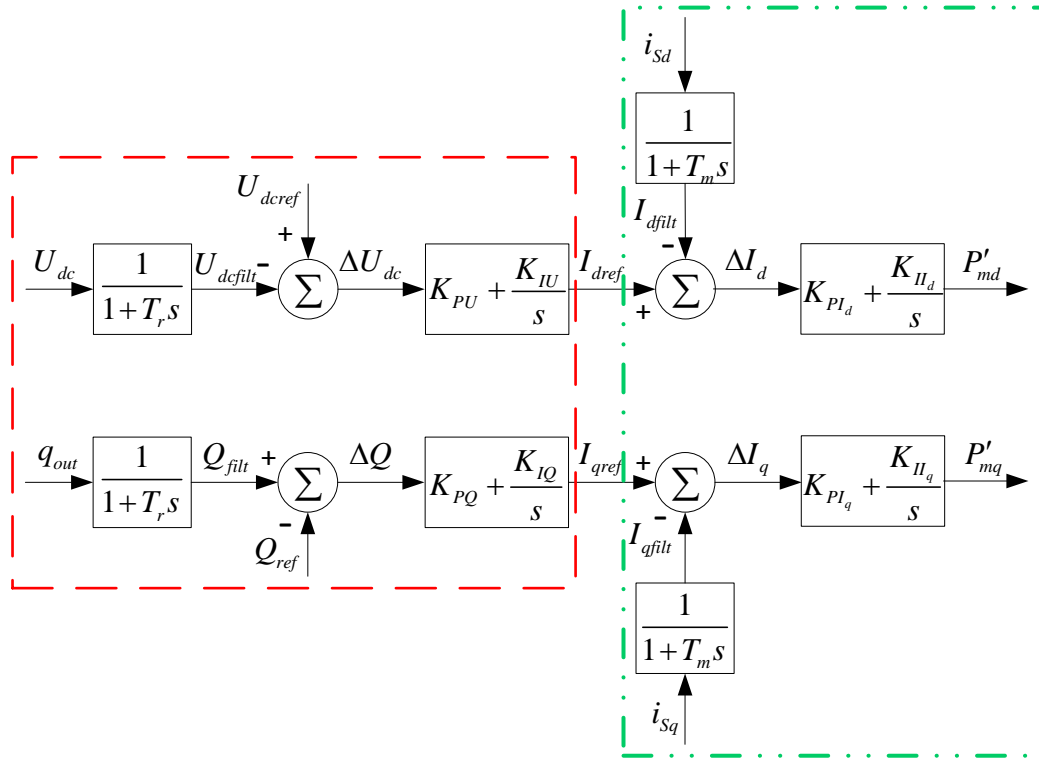
Fig. 4.1 [42].

Figure 4.1 A typical dual-loop control system

It is better to describe Fig. 4.1. There are ten unknown parameters in this system, which are T_r, T_m, K_{PU}, K_{IU}, K_{PQ}, K_{IQ}, K_{PI_d}, K_{II_d}, K_{PI_q}, K_{II_q}. The structure of it is symmetric, and the upper half part is d-axis controller and the lower half part is q-axis controller. The part in the red frame is the outer-loop controller which represents the control aim and generates reference signals for the inner-loop controller. The part in the green frame is the inner-loop controller which is used for precise adjustment of currents. The parameters T_r and T_m affect the function of filters. The parameters K_{PU} and K_{IU}, K_{PQ} and K_{IQ} are used to control U_{dc} and q_{out}, respectively. The parameters K_{PI_d}, K_{II_d}, K_{PI_q} and K_{II_q} affect the function of inner-loop controller, which is to precisely adjust the current. Therefore, the parameter identification is necessary to keep the micro-grid

stability. The micro-grid stability guarantees the power supply of the loads connected within the micro-grid. To identify all the parameters, the whole system can be divided into some small parts. These parts mainly have two types, which are the low-pass filter elements and the proportional-integral elements.

4.2 Low-Pass Filter Element

The structure of a low-pass filter element is shown in Fig. 4.2, where u and y are input and output signals, respectively. The parameter to be identified here is T. According to Fig. 4.2, the transfer function is given in (4-1).
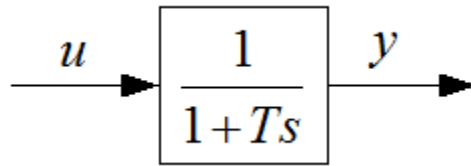
Figure 4.2 A low-pass filter element

$$y = \frac{1}{1 + Ts} u$$

$$(4\text{-}1)$$

And then, the time-domain form shown in (4-2) can be obtained based on (4-1).

$$y = \frac{u}{T}\left(1 - e^{-t/T}\right)$$

$$(4\text{-}2)$$

In this thesis, parameter identification is realized by MATLAB. Fig. 4.3 and Fig. 4.4 illustrate the result of the parameter identification of the low-pass filter element. Fig.

4.3 represents the iteration process of the parameter identification, whereas Fig. 4.4 only shows the final result. In the two figures, x-axis represents the time t and y-axis represents the values of y at different time. Set the initial value $T^{(0)} = 1.2$, and the known input $u = 1.0$. The true parameter to be identified is $T = 1$. The red points in Fig. 4.3 are sample measurements $\mathbf{f} = (f_1, f_2, f_3 \dots f_{10})$ taken from the low-pass filter element with the known input, for which sampling errors have been considered. The red curve is the y-t curve in Fig. 4.3 when T is set equal to the initial value $T^{(0)} = 1.2$. The green curves are the y-t curves during the iteration. The black curve is the final y-t curve matching the sample measurements $\mathbf{f}$ very well. The blue hollow points are the corresponding sample points in the curves $\mathbf{f_p} = (f_{p1}, f_{p2}, f_{p3} \dots f_{p10})$. In Fig. 4.4, red points represent the sample measurements $\mathbf{f} = (f_1, f_2, f_3 \dots f_{10})$. The black curve is the final y-t curve matching the sample points $\mathbf{f}$ very well. The blue hollow points are the corresponding sample points in the curves $\mathbf{f_p}^{(4)} = (f_1^{(4)}, f_2^{(4)}, f_3^{(4)} \dots f_{10}^{(4)})$. The values of $\mathbf{f}$ and $\mathbf{f_p}^{(n)}, n = 0, 1, \dots, 4$ are shown in the Table 4.1. The first column indicates the time point of each sample measurement and sample point. The second column indicates the values of sample measurements $\mathbf{f}$. The third column indicates the values of sample points $\mathbf{f_p}^{(0)}$ when T is set equal to the initial value $T^{(0)} = 1.2$. The fourth column, the fifth column, the sixth column and the seventh column are the values of sample points $\mathbf{f_p}^{(1)}$, $\mathbf{f_p}^{(2)}, \mathbf{f_p}^{(3)}$ and $\mathbf{f_p}^{(4)}$ respectively. The algorithm stops after the fourth iteration because the error is small enough.
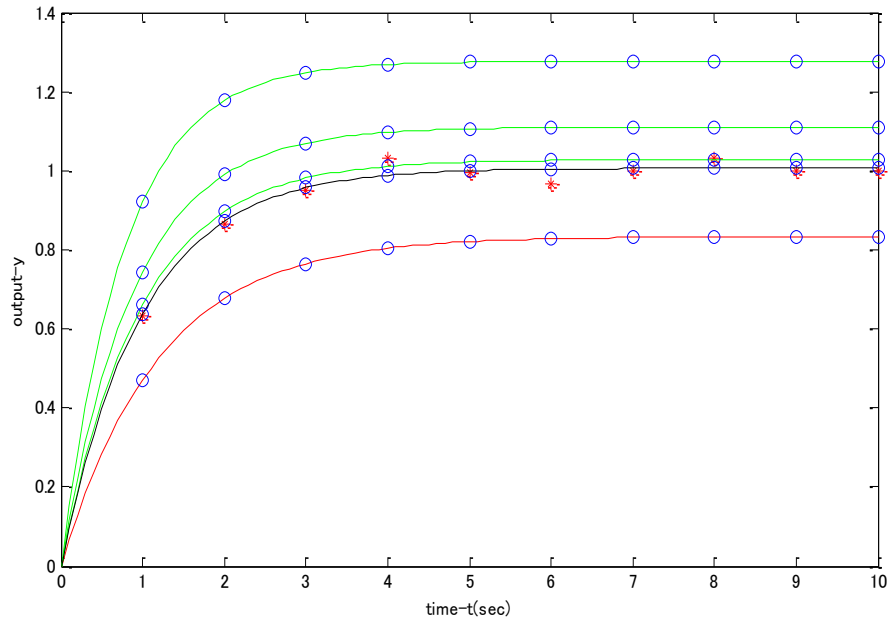
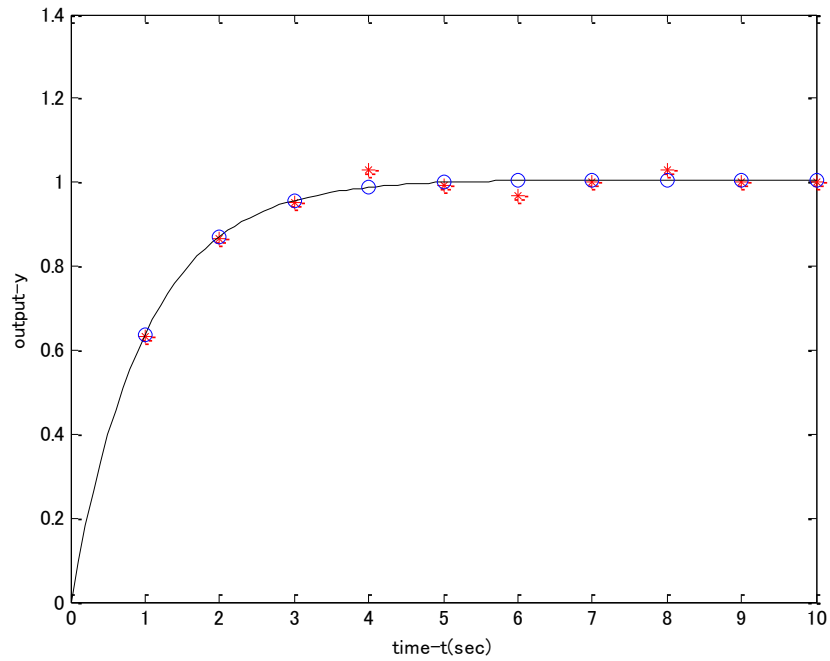**Figure 4.3 The result of parameter identification with process**

Figure 4.4 The final result of parameter identification

35

t/sec	f	$f_p^{(0)}$	$f_p^{(1)}$	$f_p^{(2)}$	$f_p^{(3)}$	$f_p^{(4)}$
1	0.6321	0.4712	0.9200	0.7441	0.6602	0.6384
2	0.8647	0.6759	1.1768	0.9893	0.8963	0.8718
3	0.9502	0.7649	1.2485	1.0702	0.9808	0.9571
4	1.0308	0.8036	1.2685	1.0968	1.0111	0.9883
5	0.9933	0.8204	1.2740	1.1056	1.0219	0.9997
6	0.9676	0.8277	1.2756	1.1085	1.0257	1.0039
7	0.9991	0.8309	1.2760	1.1094	1.0271	1.0054
8	1.0297	0.8323	1.2762	1.1098	1.0276	1.0059
9	0.9999	0.8329	1.2762	1.1099	1.0278	1.0061
10	1.0000	0.8331	1.2762	1.1099	1.0279	1.0062

Table 4.1 The values of f and f_p during iteration
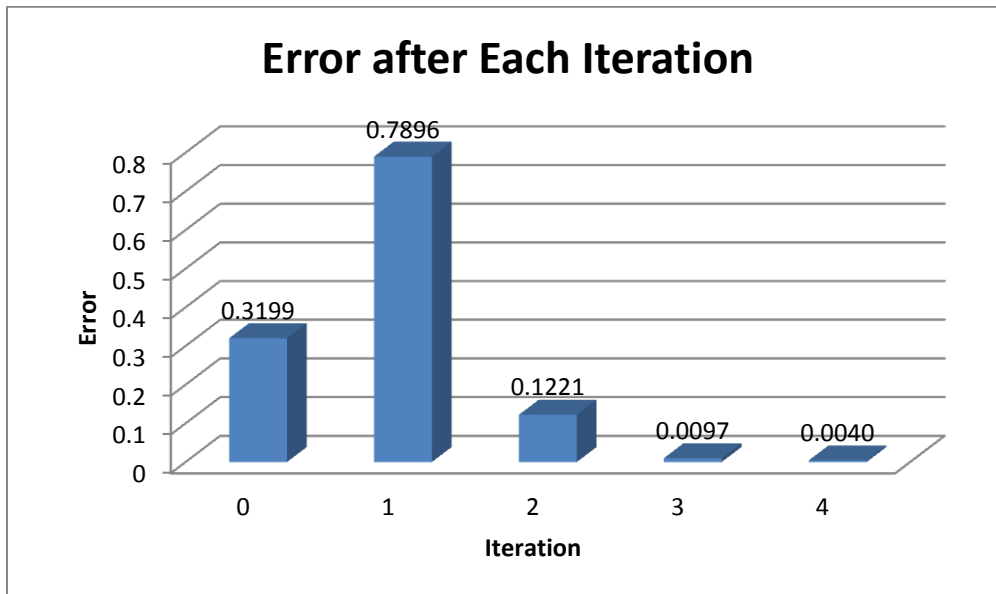
Figure 4.5 The error during iteration

36

Fig. 4.5 indicates the values of the error after every iteration. The error is the sum of squares of the differences between $\mathbf{f}_p^{(n)}$ and $\mathbf{f}$. n is the iteration times. As the figure shows, the errors generally show a descending trend, which confirms the effectiveness of the proposed approach. The iteration begins at the second bar. The first bar represents the error when T is set as the initial value $T^{(0)}$. Finally it can be seen that the error decreases to a very small value, which proves that the method can be successfully used to identify the parameter of the system. The final result is $T = 0.9938$.

4.3 Proportional-Integral Element

The structure of the proportional integral element is shown in Fig. 4.6, with u and y being the input and output signals, respectively. The parameters to be identified are T and K. According to Fig. 4.6, the frequency-domain function of y is:
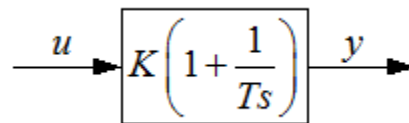
$$y = uK(1 + \frac{1}{Ts})$$

(4-3)

Figure 4.6 Proportional-integral element

The time-domain form shown in (4-4) can be obtained based on (4-3).

$$y = \frac{u}{T}t + uK$$

Fig. 4.6 and Fig. 4.7 represent the process and result of the parameter

identification of the proportional integral element. In the two figures, x-axis represents

the time t and y-axis represents the values of y at different time. Set the initial values

$T^{(0)} = 2.2$ and $K^{(0)} = 1.2$, and the known input $u = 1.0$. The true parameters to be

identified are $T = 2$ and $K = 1$. The red points in Fig. 4.6 are sample measurements

$\mathbf{f} = (f_1, f_2, f_3 \dots f_{10})$ taken from the low-pass filter element with the known input, for

which sampling errors have been considered. The red curve is the y-t curve in Fig. 4.6

when T is set equal to the initial value $T^{(0)} = 2.2$ and $K^{(0)} = 1.2$. The green curves are

the y-t curves during the iteration. The black curve is the final y-t curve matching the

sample measurements $\mathbf{f}$ very well. The blue hollow points are the corresponding sample

points in the curves $\mathbf{f_p} = (f_{p1}, f_{p2}, f_{p3} \dots f_{p10})$. In Fig. 4.7, red points represent the

sample measurements $\mathbf{f} = (f_1, f_2, f_3 \dots f_{10})$. The black curve is the final y-t curve

matching the sample points $\mathbf{f}$ very well. The blue hollow points are the corresponding

sample points in the curves $\mathbf{f_p}^{(5)} = (f_1^{(5)}, f_2^{(5)}, f_3^{(5)} \dots f_{10}^{(5)})$. Table 4.2 represents the

values of $\mathbf{f}$ and $\mathbf{f_p}^{(n)}, n = 0, 1, \dots, 5$ after every iteration. Fig. 4.8 represents the error after

every iteration. The first column indicates the time point of each sample measurement

and sample point. The second column indicates the values of sample measurements $\mathbf{f}$.

The third column indicates the values of sample points $\mathbf{f_p}^{(0)}$ when T and K are set equal to

the initial value $T^{(0)} = 2.2$ and $K^{(0)} = 1.2$. The fourth column, the fifth column, the sixth

column, the seventh column and the eighth column are the values of sample points $\mathbf{f_p}^{(1)}$,

$\mathbf{f_p}^{(2)}$, $\mathbf{f_p}^{(3)}$, $\mathbf{f_p}^{(4)}$ and $\mathbf{f_p}^{(5)}$ respectively. The iteration stops after the fifth iteration because the error is small enough. The error is indicated in Fig 4.8.
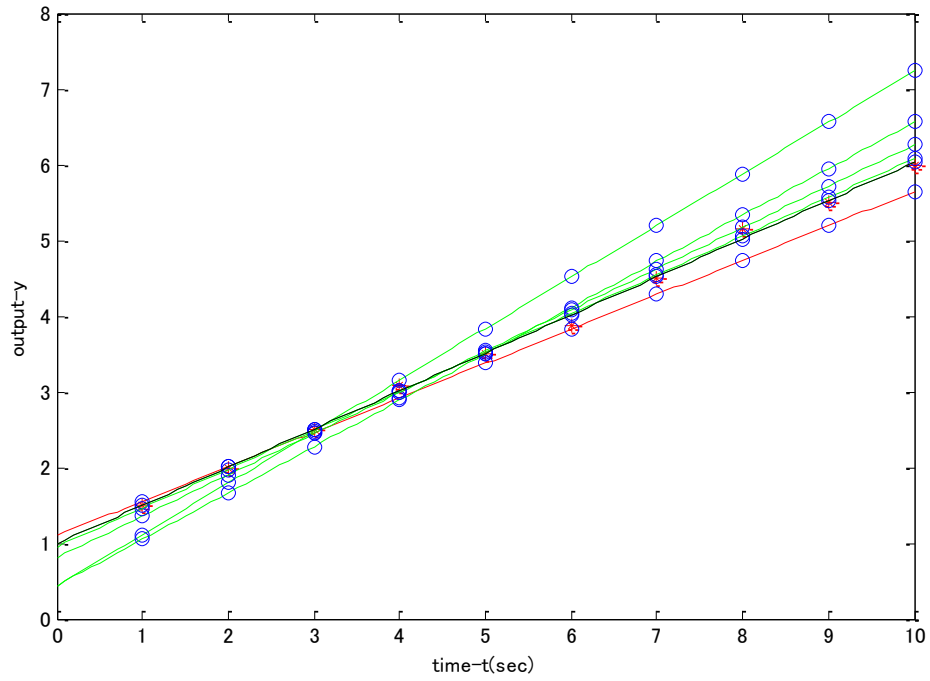

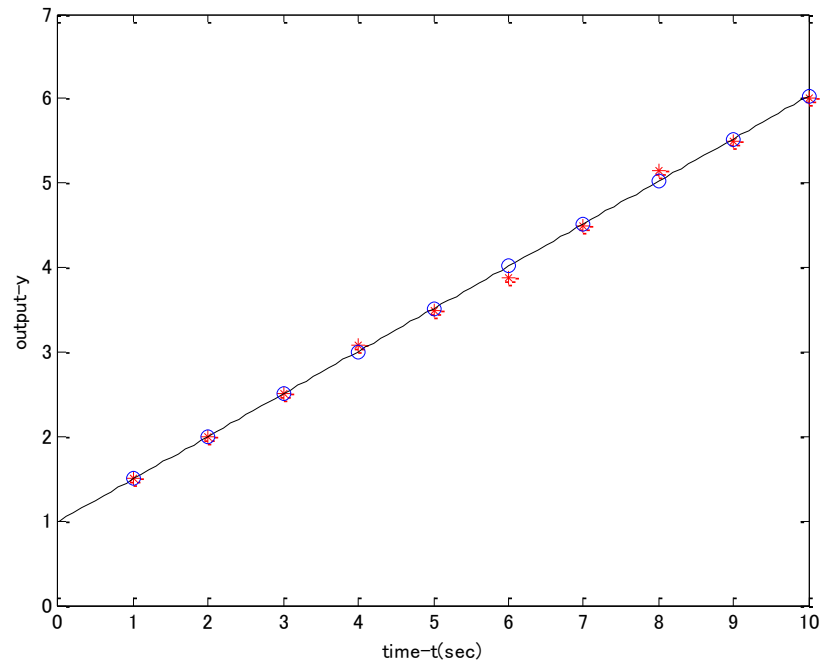**Figure 4.6 The result of parameter identification process**

Figure 4.7 The final result of parameter identification

t/sec	f	$f_p^{(0)}$	$f_p^{(1)}$	$f_p^{(2)}$	$f_p^{(3)}$	$f_p^{(4)}$	$f_p^{(5)}$
1	1.5000	1.5545	1.1117	1.0499	1.3565	1.4636	1.4991
2	2.0000	2.0091	1.7927	1.6620	1.9012	1.9767	2.0022
3	2.5000	2.4636	2.4736	2.2742	2.4460	2.4899	2.5053
4	3.0900	2.9182	3.1546	2.8863	2.9907	3.0030	3.0084
5	3.5000	3.3727	3.8356	3.4985	3.5355	3.5161	3.5115
6	3.8800	3.8273	4.5165	4.1106	4.0802	4.0293	4.0147
7	4.5000	4.2818	5.1975	4.7228	4.6250	4.5424	4.5178
8	5.1500	4.7364	5.8784	5.3349	5.1697	5.0556	5.0209

9	5.5000	5.1909	6.5594	5.9471	5.7145	5.5687	5.5240
10	6.0000	5.6455	7.2403	6.5592	6.2592	6.0818	6.0271

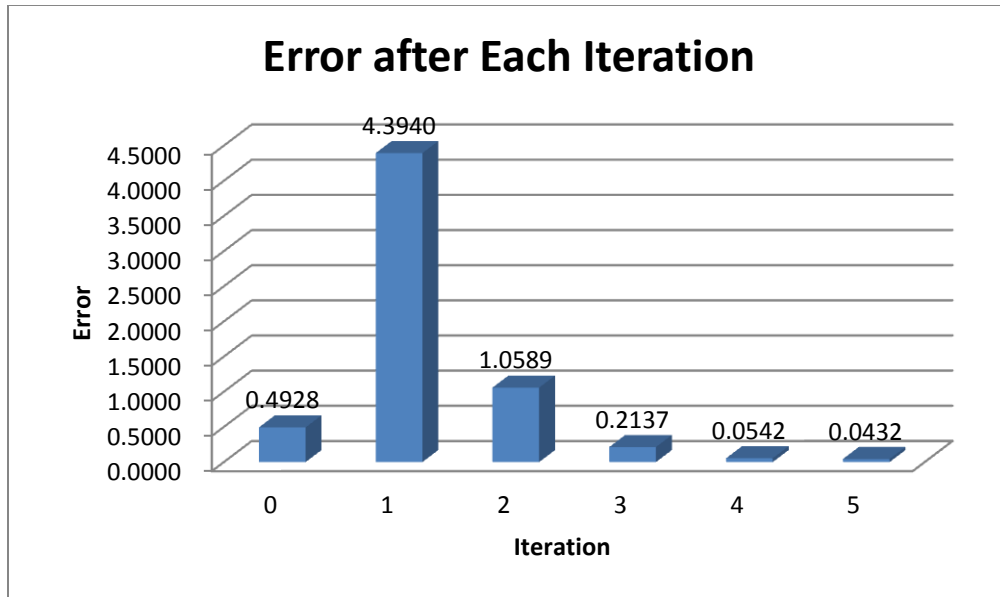**Table 4.2 The values of f and f_p during iteraton**

Figure 4.8 The error during iteration

The errors also generally show a descending trend, from which the effectiveness of the identification method can be verified as well. The final identification result is $T = 1.9877$ and $K = 0.9960$.

4.4 Parameter Identification of the Microgrid Control System

Based on the identification of two fundamental parts of the microgrid control system, the parameters of the whole control system can be identified. As shown in Fig. 4.1, the control system is symmetry in structure. Therefore, the d-axis controller can be

taken out and identified for convenience as shown in Fig. 4.9. The input signals are U_{dc}, U_{dcref} and i_{sd}. The output signal is P'_{md}. This system can be divided into three single-input-single-output (SISO) systems as shown in Fig. 4.10. The final output is the sum of the three outputs. The three systems can be identified respectively.
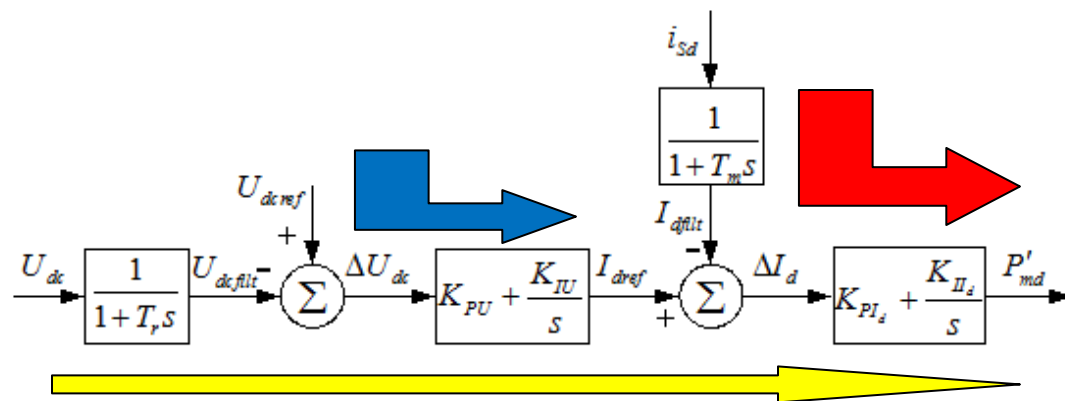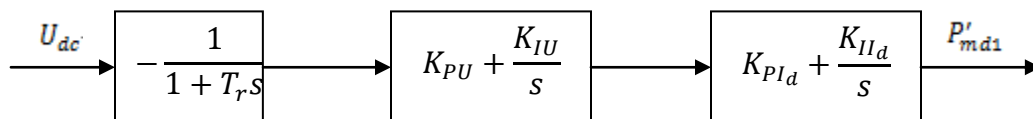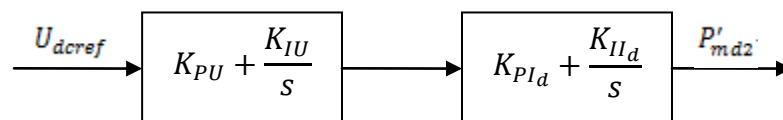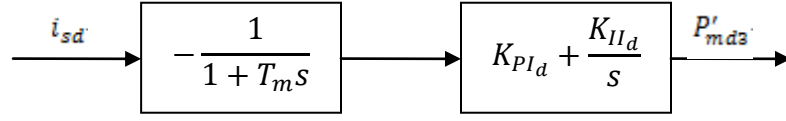
$$P'_{md} = P'_{md1} + P'_{md2} + P'_{md3} \tag{4-5}$$

Figure 4.9 d-axis controller

(a) Loop 1 of d-axis controller

(b) Loop 2 of d-axis controller

42

(c) Loop 3 of d-axis controller

Figure 4.10 Three SISO systems of d-axis controller

The time-domain function of the system represented in Fig. 4.10(a) is given as follows.

$$P'_{md1} = -\frac{U_{dc}}{T_r}\left(1 - e^{-\frac{t}{T_r}}\right)\left[\frac{K_{IU}K_{II_d}}{K_{PU}K_{PI_d}}t^2 + \left(\frac{K_{PU}K_{II_d}}{K_{PI_d}} + \frac{K_{IU}K_{PI_d}}{K_{PU}}\right)t + K_{PU}K_{PI_d}\right]$$

$$(4\text{-}6)$$

The parameter identification process of this loop is shown in Fig. 4.11 and Fig. 4.12. Fig. 4.11 represents the whole process during identification, and Fig. 4.12 only represents the final results. Set the initial values $T_r = 0.9$, $K_{PU} = 0.9$, $K_{IU} = 0.4$, $K_{PI_d} = 1.9$, $K_{II_d} = 0.9$, and the known input $U_{dc} = 1.0$. In Fig. 4.11, the red points are the sample measurements **f**. The green curves are the y-t curves during the iteration including the initial one and the final one. The blue hollow points are sample points of these green curves. In Fig. 4.12, the red points are the sample measurements **f**. The green curve is the final y-t curve matching the sample measurements **f** very well. The blue hollow points are sample points of the green curve. The true parameters to be identified are $T_r = 1.0$, $K_{PU} = 1.0$, $K_{IU} = 0.5$, $K_{PI_d} = 2.0$, and $K_{II_d} = 1.0$. The final values of the parameters are $T_r = 1.0293$, $K_{PU} = 1.1005$, $K_{IU} = 0.4973$, $K_{PI_d} = 1.9618$, and $K_{II_d} = 0.9156$.

43

The time-domain function of the system represented in Fig. 4.10(b) is as follows.

$$P'_{md2} = U_{dcref} \left[\frac{K_{IU}K_{II_d}}{K_{PU}K_{PI_d}} t^2 + \left(\frac{K_{PU}K_{II_d}}{K_{PI_d}} + \frac{K_{IU}K_{PI_d}}{K_{PU}} \right) t + K_{PU}K_{PI_d} \right]$$

(4-7)

The parameter identification process of this loop is shown in Fig. 4.13 and Fig. 4.14. Fig. 4.13 represents the whole process during identification and Fig. 4.14 only represents the final results. Set the initial values $K_{PU} = 1.2$, $K_{IU} = 0.7$, $K_{PI_d} = 2.2$, $K_{II_d} = 1.2$, and the known input $U_{dcref} = 1.0$. In Fig. 4.13, the red points are the sample measurements **f**. The green curves are the y-t curves during the iteration including the initial one and the final one. The blue hollow points are sample points of these green curves. In Fig. 4.14, the red points are the sample measurements **f**. The green curve is the final y-t curve matching the sample measurements **f** very well. The blue hollow points are sample points of the green curve. The true parameters to be identified are $K_{PU} = 1.0$, $K_{IU} = 0.5$, $K_{PI_d} = 2.0$, and $K_{II_d} = 1.0$. The final values of the parameters are $K_{PU} = 1.0333$, $K_{IU} = 0.5433$, $K_{PI_d} = 1.9220$, and $K_{II_d} = 0.9156$.

The time-domain function of the system represented in Fig. 4.10(c) is expressed as follows

$$P'_{md3} = -\frac{i_{sd}}{T_m} \left(1 - e^{-\frac{t}{T_m}} \right) \left(\frac{K_{II_d}}{K_{PI_d}} t + K_{PI_d} \right)$$

(4-8)

The parameter identification process of this loop is shown in Fig. 4.15 and Fig. 4.16. Fig. 4.15 represents the whole process during identification, and Fig. 4.16 only represents the final identification results. Set the initial values $T_m = 1.2$, $K_{PI_d} = 2.2$, $K_{II_d} = 1.2$, and the known input $i_{sd} = 1.0$. In Fig. 4.15, the red points are the sample measurements $\mathbf{f}$. The green curves are the y-t curves during the iteration including the initial one and the final one. The blue hollow points are sample points of these green curves. In Fig. 4.16, the red points are the sample measurements $\mathbf{f}$. The green curve is the final y-t curve matching the sample measurements $\mathbf{f}$ very well. The blue hollow points are sample points of the green curve. The true parameters to be identified are $T_m = 1.0$, $K_{PI_d} = 2.0$, and $K_{II_d} = 1.0$. The final values of the parameters are $T_m = 1.0343$, $K_{PI_d} = 2.0888$, and $K_{II_d} = 1.0790$.
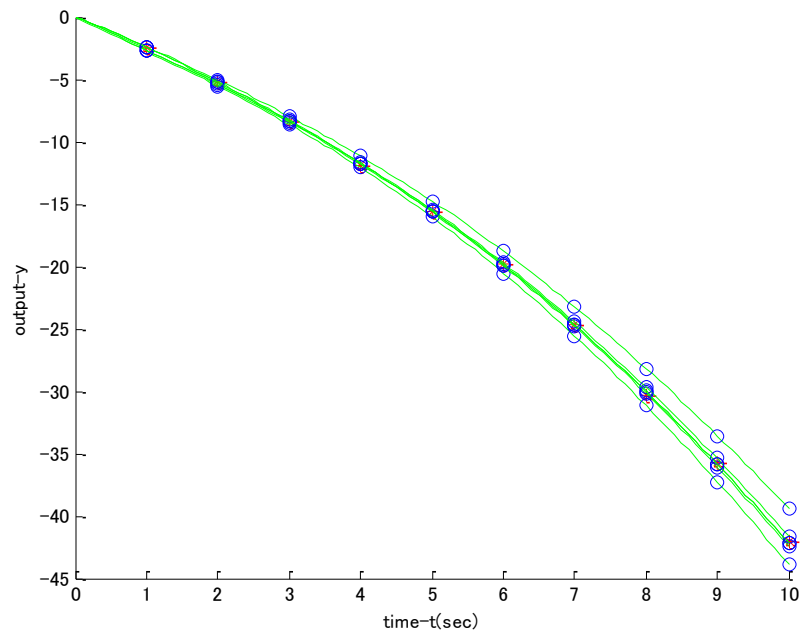

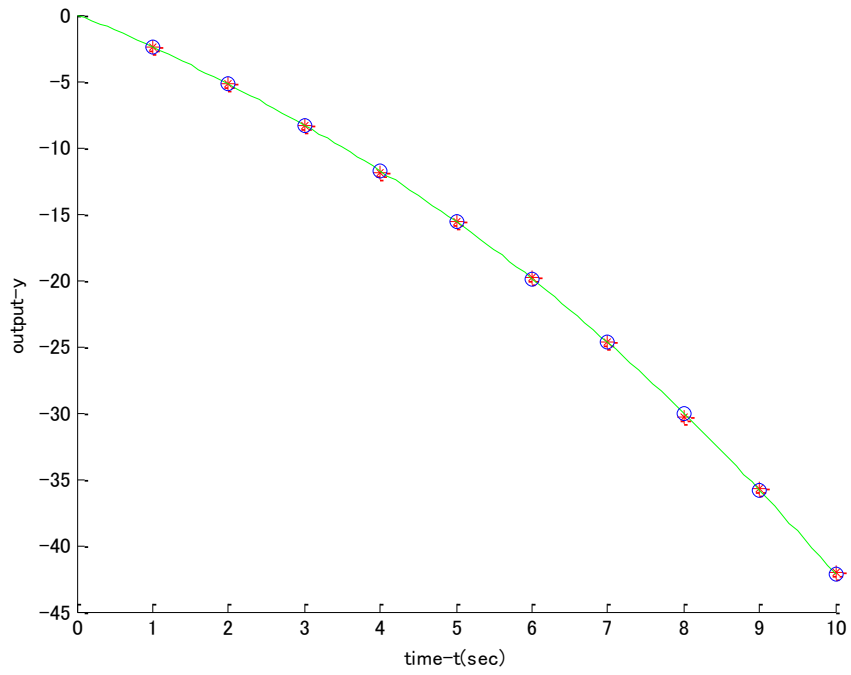**Figure 4.11 The result of parameter identification process**

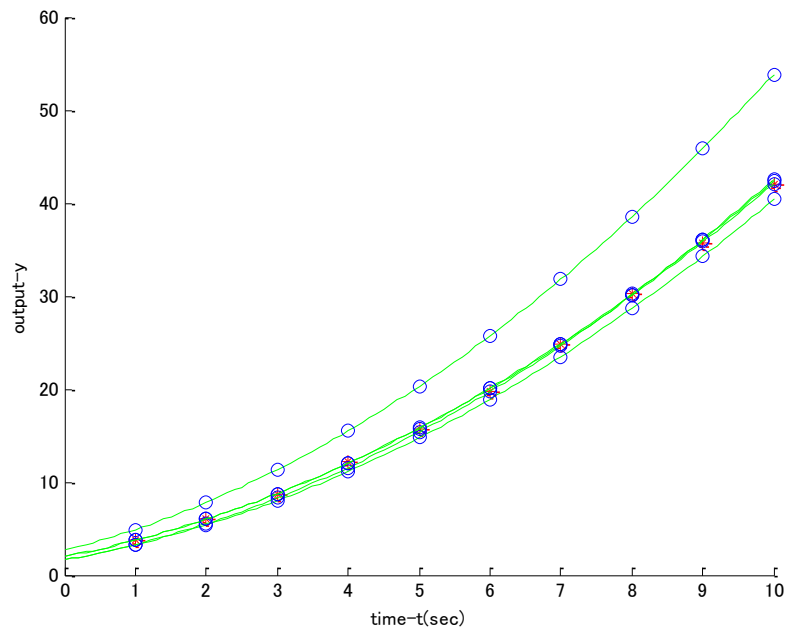**Figure 4.12 The final result of parameter identification**

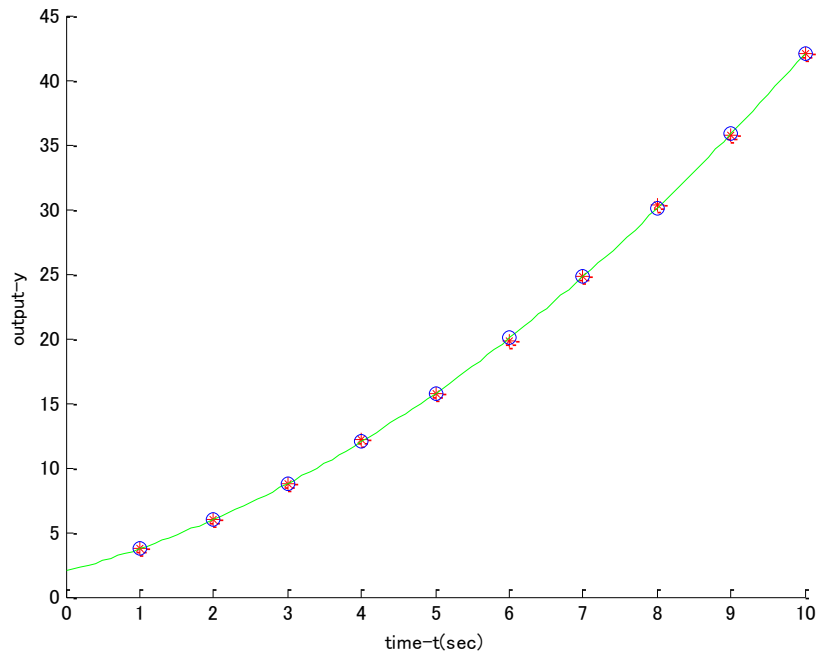**Figure 4.13 The result of parameter identification process**

46

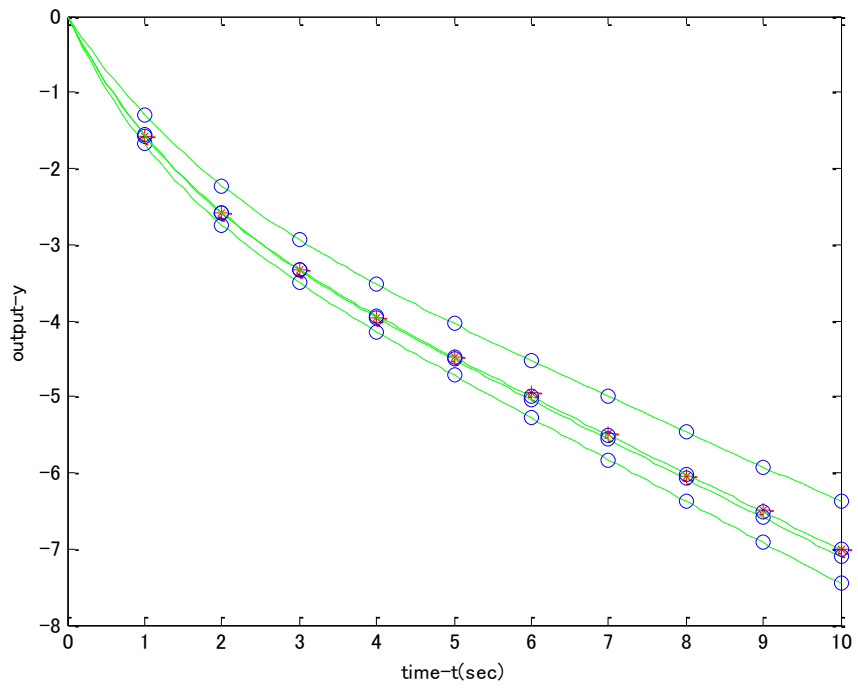**Figure 4.14 The final result of parameter identification**

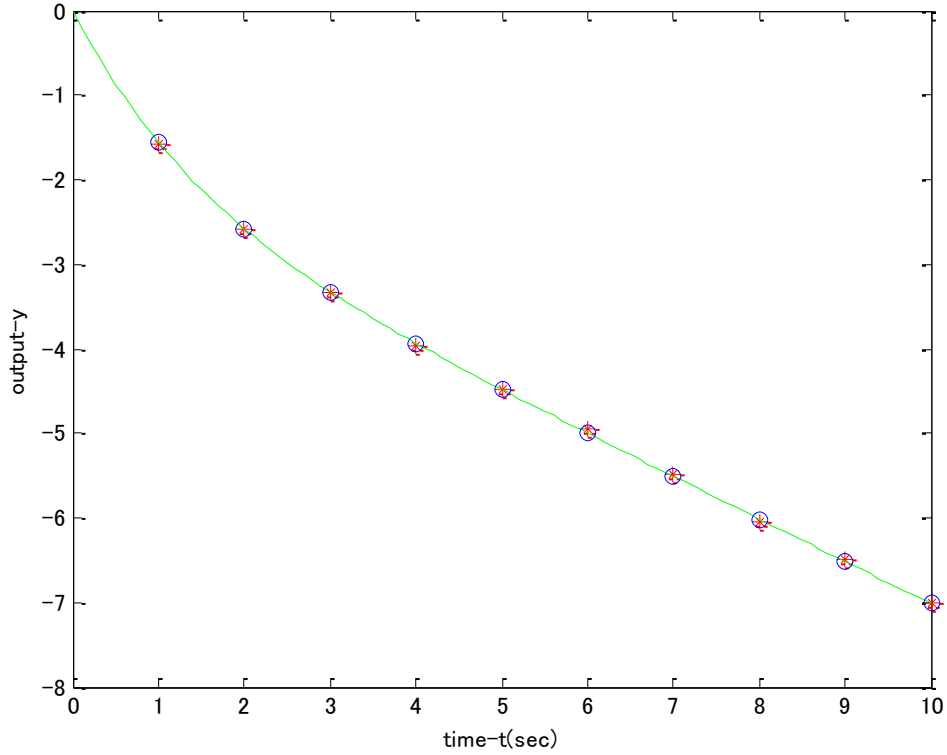**Figure 4.15 The result of parameter identification process**

Figure 4.16 The final result of parameter identification

According to equation (4-5), the function of the control system represented in Fig. 4.9 can be obtained.

$$P'_{md} = \left[U_{dcref} - \frac{U_{dc}}{T_r}\left(1 - e^{-\frac{t}{T_r}}\right) \right] \left[\frac{K_{IU}K_{II_d}}{K_{PU}K_{PI_d}} t^2 + \left(\frac{K_{PU}K_{II_d}}{K_{PI_d}} + \frac{K_{IU}K_{PI_d}}{K_{PU}} \right) t + K_{PU}K_{PI_d} \right]$$

$$- \frac{i_{sd}}{T_m}\left(1 - e^{-\frac{t}{T_m}}\right)\left(\frac{K_{II_d}}{K_{PI_d}} t + K_{PI_d} \right)$$

(4-9)

The parameter identification process is shown in Fig. 4.17 and Fig. 4.18. Fig. 4.17

represents the whole process during identification, and Fig. 4.18 only represents the final

results. Set the initial values $T_r = 0.9$, $T_m = 1.1$, $K_{PU} = 0.9$, $K_{IU} = 0.6$, $K_{PI_d} = 1.9$,

$K_{II_d} = 0.9$, and the known input $U_{dc} = 1.0$, $U_{dcref} = 1.0$, $i_{sd} = 1.0$. In Fig. 4.17, the red

points are the sample measurements **f**. The green curves are the y-t curves during the

iteration including the initial one and the final one. The blue hollow points are sample

points of these green curves. In Fig. 4.18, the red points are the sample measurements **f**.

The green curve is the final y-t curve matching the sample measurements **f** very well.

The blue hollow points are sample points of the green curve. The true parameters to be

identified are $T_r = 1.0$, $T_m = 1.0$, $K_{PU} = 1.0$, $K_{IU} = 0.5$, $K_{PI_d} = 2.0$, and $K_{II_d} = 1.0$.

The final values of the parameters are $T_r = 0.9247$, $T_m = 1.1917$, $K_{PU} = 1.3275$,

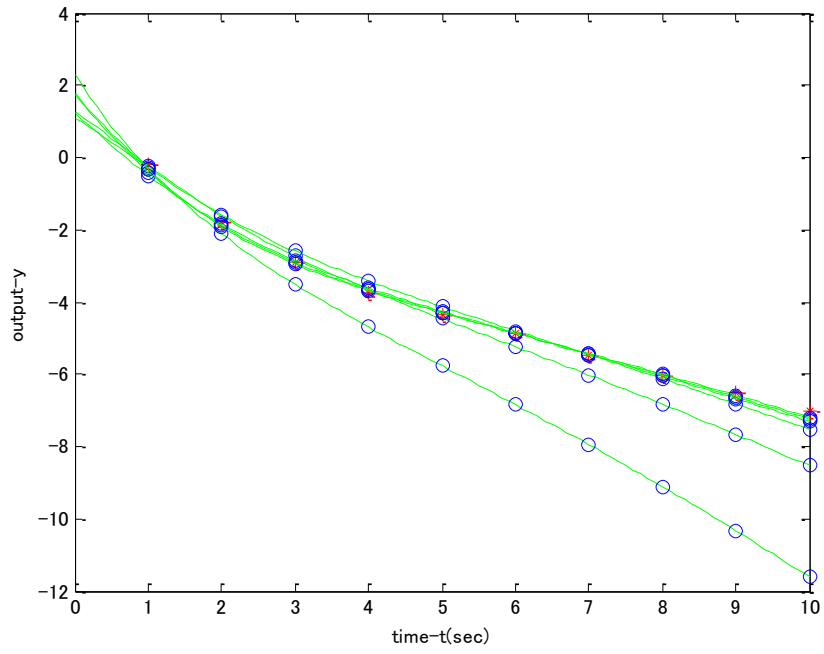$K_{IU} = 0.4371$, $K_{PI_d} = 2.3720$, and $K_{II_d} = 0.8283$.

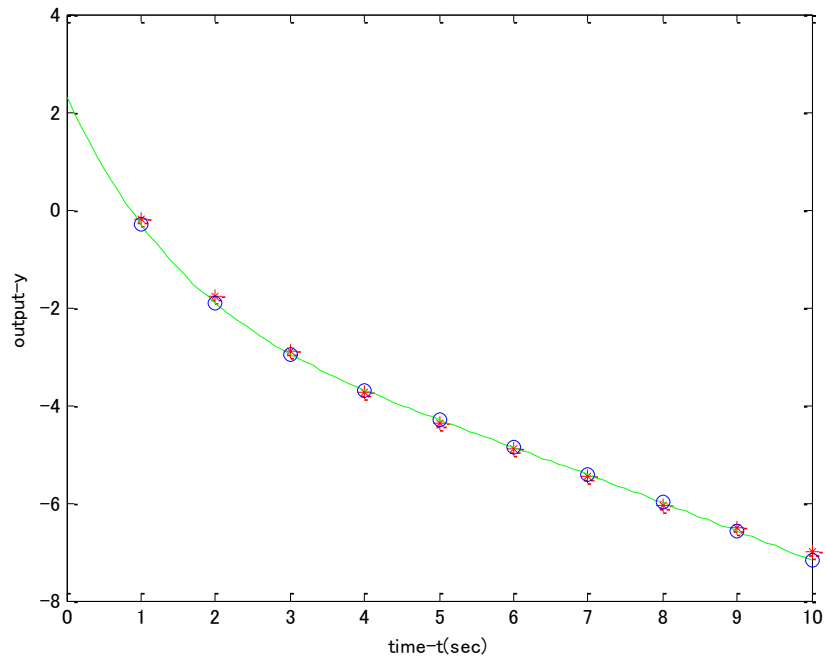**Figure 4.17 The result of parameter identification process**

Figure 4.18 The final result of parameter identification

The function of the other half of the control system in the q-axis can also be obtained.

$$P'_{mq} = \left[\frac{q_{out}}{T_r}\left(1 - e^{-\frac{t}{T_r}}\right) - Q_{ref}\right]\left[\frac{K_{IQ}K_{II_q}}{K_{PQ}K_{PI_q}}t^2 + \left(\frac{K_{PQ}K_{II_q}}{K_{PI_q}} + \frac{K_{IQ}K_{PI_q}}{K_{PQ}}\right)t + K_{PQ}K_{PI_q}\right]$$

$$-\frac{i_{sq}}{T_m}\left(1 - e^{-\frac{t}{T_m}}\right)\left(\frac{K_{II_q}}{K_{PI_q}}t + K_{PI_q}\right)$$

(4-10)

The parameter identification process is shown in Fig. 4.19 and Fig. 4.20. Fig. 4.19 represents the whole process during identification, and Fig. 4.20 only represents the final results. Set the initial values $T_r = 0.9$, $T_m = 1.1$, $K_{PQ} = 0.9$, $K_{IQ} = 0.4$, $K_{PI_q} = 1.9$, $K_{II_q} = 0.9$, and the known input $q_{out} = 1.0$, $Q_{ref} = 1.0$, $i_{sq} = 1.0$. In Fig. 4.19, the red points are the sample measurements $\mathbf{f}$. The green curves are the y-t curves during the iteration including the initial one and the final one. The blue hollow points are sample points of these green curves. In Fig. 4.20, the red points are the sample measurements $\mathbf{f}$. The green curve is the final y-t curve matching the sample measurements $\mathbf{f}$ very well. The blue hollow points are sample points of the green curve. The true parameters to be identified are $T_r = 0.5$, $T_m = 0.4$, $K_{PQ} = 1.5$, $K_{IQ} = 0.5$, $K_{PI_q} = 2.0$, and $K_{II_q} = 1.0$. The final values of the identified parameters are $T_r = 0.4360$, $T_m = 0.3186$, $K_{PQ} = 1.4663$, $K_{IQ} = 0.4134$, $K_{PI_q} = 1.9276$, and $K_{II_q} = 0.9024$.
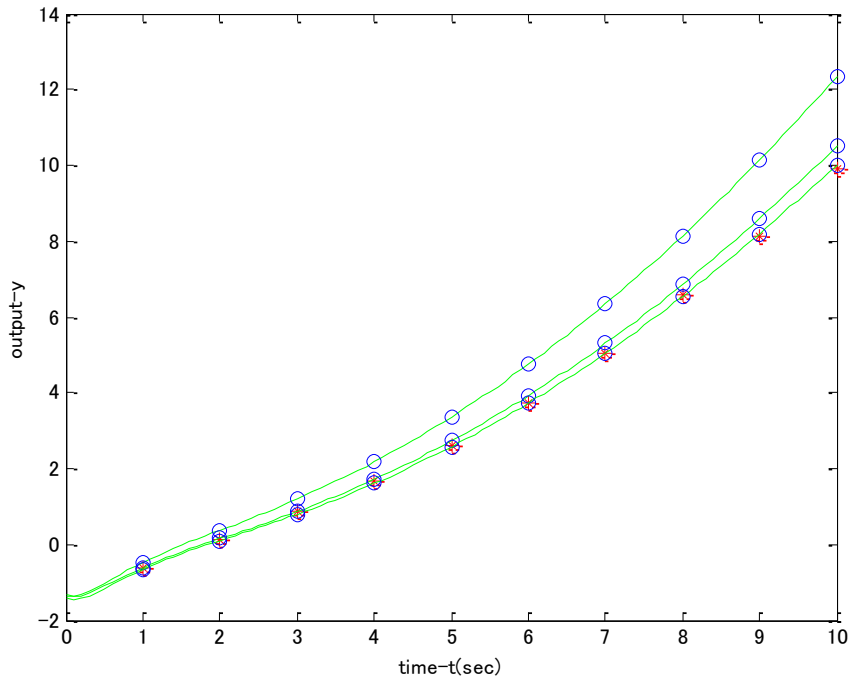
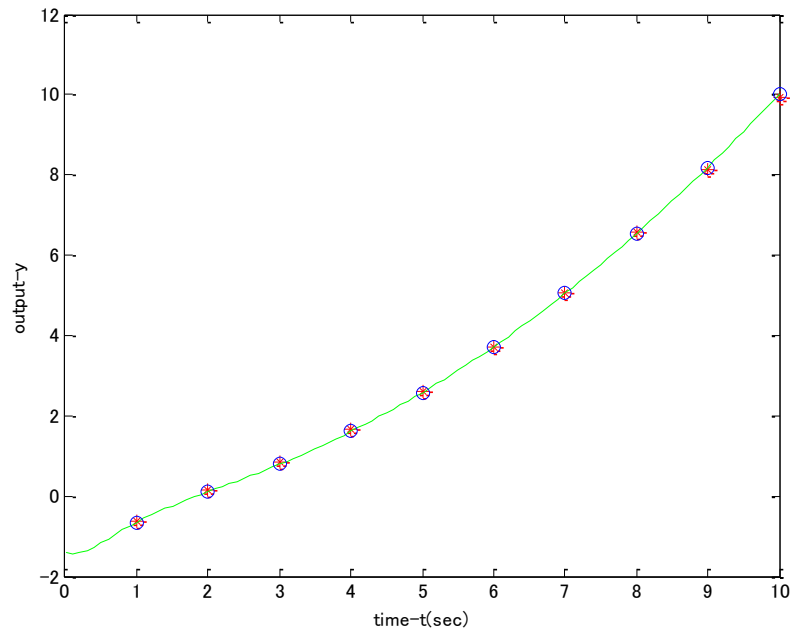**Figure 4.19 The result of parameter identification process**

Figure 4.20 The final result of parameter identification

Table 4.3 shows the operating performance of the algorithm. The first column indicates the types of elements or systems that are studied the parameter identification in my thesis. The second column represents the iteration times of each program. The third column represents the computation time of each program. The fourth column represents the sum of squares of differences between the sample points and the sample measurements of each element or system.

System Type	Iteration Times	Computation Time (sec)	Error
Low-Pass Filter	4	1.076	0.0040
Proportional Integral	5	2.977	0.0432
Loop 1	5	123.776	0.1587
Loop 2	4	45.113	0.1372
Loop 3	3	16.899	0.0084
d-axis Controller	5	182.687	0.0865
q-axis Controller	2	87.959	0.0316

Table 4.3 The operating performance of the algorithm

Table 4.4 shows the errors after different iteration times. The first column represents the system types. The second column shows the errors of parameter identification of the four types of systems obtained in my thesis, which have been shown in Column 4 of Table 4.3. The third column shows the errors of parameter identification of the four types of systems after 40 times iteration with the same method, in order to

prove whether increasing iteration times can enhance the accuracy of the results. The

errors of the low-pass filter element and the proportional integral element do not change

after 40 times iteration, which indicates that we have obtained the best results after a few

iteration steps as indicated in Column 2 of Table 4.3. More iteration is not necessary. The

errors of the d-axis controller and the q-axis controller are very big after 40 times

iteration. The reason of it is that during iteration, when very good results are obtained, the

Jacobian matrix will be very close to singular. It seriously influences the computation and

makes the results useless. It also indicates that more iteration is not needed. Therefore,

more iteration cannot improve the accuracy of the results.

System Type	Error (Column 4 of Table 4.3)	Error after 40 Times Iteration
Low-Pass Filter	0.0040	0.0040
Proportional Integral	0.0432	0.0432
d-axis Controller	0.0865	Infinite
q-axis Controller	0.0316	Infinite

Table 4.4 The error after different iteration times

Chapter 5: Conclusion and Future Work

5.1 Conclusion

Many parameters of the micro-grid need to be identified. These parameters are critical to the stability of the micro-grid. "parameter identification of the micro-grid control system" is analyzed and investigated in this thesis, involving the following three parts.

(1) System parameter identification is to estimate the parameters based on the known system structure, and the tools used are the least squares method and Newton-Raphson algorithm. The least squares method is to judge whether the parameters reach the requirement during iteration, and according to different situation the least squares method can also be divided into several types, such as weighed least squares method and recursive least squares method. algorithm is used to update the values of parameters to reach the requirement. The core of Newton-Raphson is computation of Jacobian Matrix.

(2) One of the most important parts of a micro-grid is the control system. The micro-grid can run in grid-connected operation mode or islanded operation mode. The process of mode transition between the two modes needs to be smooth to ensure the micro-grid stability. The micro-grid stability is important to the power supply of the loads connected within the micro-grid. The control system is critical to keep the process smooth, and the corresponding parameters are responsible for disturbance suppression.

(3) Finally the thesis introduces the model of a common control system called inverter dual-loop control system. To identify the parameters of it, the parameters of the low-pass filter element and the proportional integral element are firstly identified by this method. Then system identification of the whole control system can be divided into d-axis controller and q-axis controller. The two controllers' structures are symmetric. One controller is a three-input-single-output system. It can be also divided into three SISO systems for the system identification to be done respectively. Finally the system identification of the two controllers is obtained.

Therefore, this kind of method which combines the least squares method with Newton-Raphson algorithm can be used for parameter identification of different types of systems. The method can identify multiple parameters at the same time and has fast convergence. It can also be reasonably realized.

5.2 Future Work

The thesis provides a method to do the parameter identification of a system. This method has general application and fast convergence. However, taking into account the selection limitation of initial values in Newton-Raphson algorithm, other methods with strong robustness characteristics (e.g., Gaussian method) can be combined as well to obtain better results of system identification. On the other hand, in this thesis, parameter identification is based on time-domain functions. Some other methods also need to be found to do the parameter identification based on frequency-domain functions. This can make the method more universal.

Of course, to identify a complex system, only parameter identification is usually not enough. The structure identification is needed as well. Therefore, next step of this work is to find a practical method to conduct the structure identification and to integrate the methods of structure identification and parameter identification. In this way, the structures and the parameters of the micro-grid can be more clear, which make it easier to design and analyze the micro-grid system or to maintain the stability of the micro-grid.

References

[1]   M. H Ashourian, A. A Mohd Zin, A. S. Mokhtar, S. J Mirazimi, Z. Muda, "Controlling and Modeling Power-Electronic Interface DERs in Islanding Mode Operation Micro Grid," *IEEE Symposium on Industrial Electronics and Applications (ISIEA),* 2011.

[2]   Haiyang Zhang, Sande Li, "Research on Micro-grid," *Advanced Power System Automation and Protection (APAP),* 2012.

[3]   Zhaoyun Zhang, Yanxin Li, Wei Chen, "The Research on Micro-grid Mode Conversion," *China International Conference on Electricity Distribution (CICED),* 2012.

[4]   Ahshan, R., Igbal, M. T., Mann, G. K. I., Quaicoe, J. E., "Micro-grid System Based on Renewable Power Generation Units," *Canadian Conference on Electrical and Computer Engineering (CCECE),* 2010.

[5]   W. Gao, V. Zheglov, G. Wang, Satish M. Mahajan, "PV-Wind-Fuel Cell-Electrolyzer Micro-grid Modeling and Control in Real Time Digital Simulator," 2009.

[6]   Weiqing Tao, Wen Sun, Chen Du, "Research on Super-Capacitor and Battery Hybrid Energy Storage System Applied in Micro-grid," *International Conference on Control Engineering and Communication Technology (ICCECT),* 2012.

61

[7] Alegria, E., Brown, T., Minear, E., Lasseter, R. H., "CERTS Microgrid Demonstration with Large-Scale Energy Storage and Renewable Generation," *IEEE Transactions on Smart Grid,* Vol. 5, no. 2, pp. 937-943, 2014.

[8] Christian Klumpner, Greg Ahser, Z. Chen, "Selecting the Power Electronic Interface for a Supercapattery Based Energy Storage System," *IEEE Bucharest Power Tech Conference,* 2009.

[9] Yan Chen, *Power System Stability Analysis,* Beijing, China Electric Power Press.

[10] A. G. Madureira, J. C. Pereira, N. J. Gil, J. A. Pecas Lopes, G. N Korres, N. D. Hatziargyriou, "Advanced Control and Management Functionalities for Multi-Microgrids," *European Transactions on Electrical Power,* 2011.

[11] Hong Zhao, Guiping Zhu, Cheng Xu, "A Novel Frequency Control Strategy of Micro-Source Based on the Secondary Frequency Regulation of Power System," *China International Conference on Electricity Distribution (CICED),* 2012.

[12] Jian Chen, Zhengyou He, Wei Jiang, "The Overview of Protection Schemes for Distribution Systems Containing Micro-Grid," *Asia-Pacific Power and Energy Engineering Conference (APPEEC),* 2011.

[13] Zhongzhou Li, Yongli Li, Guibin Fu, Botong Li, "Directional Protection Based on Fault Component Energy Function in Micro-grid," *Innovative Smart Grid Technologies – Asia (ISGT – Asia),* 2012.

[14]   Lasseter, R. H., "CERTS Microgrid," *IEEE International Conference on System of Systems Engineering,* 2007.

[15]   Earthing System, http://en.wikipedia.org/wiki/Earthing_system. Accessed on February 26, 2014.

[16]   Ilic, B., Adamovic, Z., Savic, B., Stankovic, N., "Dangares of Stray Current to Information and Communication Technologies in Electrical Installations with TN-C-S system of Distribution," *Telecommunications Forum (TELFOR),* 2011.

[17]   Rouyi Chen, Jianbin Chen, Jinyong Lei, Chao Fu, Ke Wang, Weiguo Duan, Xuzhi Dong, Guanglin Cai, "System Stability and Its Influencing Factors Analysis of the Isolated Wind-Solar-Diesel-Battery Hybrid Micro-grid," *China International Conference on Electricity Distribution (CICED),* 2012.

[18]   Wei Hu, Jianjun Sun, Minghai Gao, Xiaoming Zha, Fei Liu, Chang Lin, Weiwei Ma, "Modeling and Simulation of Micro-grid Including Inverter-Interfaced Distributed Resources Based on Dynamic Phasors," *International Future Energy Electronics Conference (IFEEC),* 2013.

[19]   Azmy, A. M., Erlich, I., "Impact of Distributed Generation on the Stability of Electrical Power System," *IEEE Power Engineering Society General Meeting,* 2005.

[20]   A. Kahrobaeian, Yasser A. R. I. Mohamed, "Stability Analysis and Control of

          Medium Voltage Micro-Grids with Dynamic Loads," Department of Electrical

          Engineering, University of Alberta, AB, Canada, 2013.

[21]   Li Yu, An Luo, Chunming Tu, Fei Rong, Shuangjian Peng, "A Micro Power Quality

          Management Technology Based on Grid-Connected Inverter," *China International*

          Conference on Electricity Distribution (CICED), 2012.

[22]   Wenxia Zuo, Pengsen Li, Xike Wu, Junzhao Cheng, "Development and

          Technologies of Micro-grid," *China Electric Power,* vol. 42, no. 7, pp. 27-29, 2009.

[23]   Tenti, P., Trombetti, D., Costabeber, Alessandro, Mattavelli, P., "Distribution Loss

          Minimization by Token Ring Control of Power Electric Interfaces in Residential

          Micro-grid," *IEEE International Symposium on Industrial Electronics (ISIE),* 2010.

[24]   Li Fu, Pengfei Li, "The Research Survey of System Identification Method,"

          International Conference on Intelligent Human-Machine System and Cybernetics

          (IHMSC), 2013.

[25]   Geoffery A. Williamson, "Linear in the Parameters Identification for Classes of

          Systems," *Conference on Decision and Control,* 1993.

[26]   Songwu Lu, Tamer Basar, "Robust Nonlinear System Identification Using Neural-

          Network Models," *IEEE Transaction on Neural Networks,* Vol. 9, no. 3, pp. 407-408,

          1998.

[27]   Mohan, B. M., Datta, K. B., "Identification via Fourier Series for a Class of Lumped and distributed parameter systems," *IEEE Transaction on Circuits and Systems,* Vol. 36, no. 11, pp. 1454-1458, 1989.

[28]   Ruilan Liu, Wei liu, "Frequency-domain Parameter Identification of Nonlinear Generator Excitation System Based on Improved Particle Filtering Algorithm," *World Congress on Intelligent Control and Automation (WCICA),* 2012.

[29]   Ren Zhen, G. G. Zhu, "Multirate Closed-loop System identification of a Variable Valve Timing Actuator for an Internal Combustion Engine," *American Control Conference (ACC),* 2010.

[30]   Zhengming Zhao, Fungshi Zheng, Jide Gao, Longya Xu, "A Dynamic On-line Parameter Identification and Full Scale System Experimental Verification for Large Synchronous Machines," *IEEE Transaction on Energy Conversion,* Vol. 10, no. 3, pp. 392-398, 1995.

[31]   Xinbo Ai, Zhongyi Zhang, "System Structure Identification by Analyzing Elements Behavior Sequences with GRA-Based ISM," *IEEE International Conference on Grey Systems and Intelligence Services (GSIS),* 2009.

[32]   Ogunfunmi, T., Chang, S. L., "Second-Order Adaptive Volterra System Identification Based on Discrete Nonlinear Wiener Model," *IEEE Proceedings of Vision, Image and Signal Processing,* Vol. 148, no. 1, pp. 21-29, 2001.

[33]   Paleologu, C., Benesty, J., Ciochina, S., "A Robust Variable Forgetting Factor Recursive Least-Squares Algorithm for System Identification," *IEEE Signal Processing Letters,* Vol. 15, pp. 597-600, 2008.

[34]   Dan Simon, *Optimal State Estimation,* Hoboken, NJ, John Wiley & Sons, Inc.

[35]   Sebe, N., Lew, M. S., "Maximum Likelihood Stereo Matching," *International Conference on Pattern Recognition,* 2000.

[36]   C. Bruno, C. Candia, L. Franchi, G. Giannuzzi, M. Pozzi, R. Zaottini, M. Zaramella, "Possibility of Enhancing Classical Weighted Least Squares State Estimation with Linear PMU Measurements," *IEEE Bucharest Power Tech Conference,* 2009.

[37]   Xuran Wang, Hongbin Sun, Boming Zhang, Wenchuan Wu, Qilai Guo, "Real-Time Local Voltage Stability Monitoring Based on PMU and Recursive Least Square Method with Variable Forgetting Factors," *IEEE Power and Energy Society Innovative Smart Grid Technologies Asia (PES ISGT Asia),* 2012.

[38]   Adi Ben-Israel, "A Newton-Raphson Method for the Solution of Systems of Equations," *Journal of Mathematical Analysis and Applications,* Vol. 15, no. 2, pp. 243-252, 1966.

[39]   S. W. Ng, Y. S. Lee, "Variable Dimension Newton-Raphson Method," *IEEE Transaction on Circuits and Systems,* Vol. 47, no. 6, pp. 809-817, 2000.

[40] Qi Wei, Xintao Liang, Changyuan Liu, Tingzhi Nie, "Research on the Combined Control Method for Parallel Inverters Control of Micro-grid," College of Electrical and Electronic Engineering, Harbin University of Science and Technology, Harbin, China, 2013.

[41] Biying Ren, Xiangqian Tong, Sha Tian, Xiangdong Sun, "Research on the Control Strategy of Inverters in the Micro-grid," Department of Electrical Engineering, Xi'an University of Technology, Xi'an, China, 2010.

[42] Chengshan Wang, Yan Li, Ke Peng, "Review of the Typical Control Method of Distributed Sources Grid-Connected Inverters," *Proceedings of CSU-EPSA,* Vol. 24, no. 2, pp. 1-9, 2012.